MSc Environomical Pathways for Sustainable Energy Systems - SELECT

MSc Thesis

POWER HARDWARE IN THE LOOP LABORATORY SETUP

Author: Viyathukattuva Mohamed Ali Mohamed Mansoor

Supervisors:

Principal supervisor: Dr Oriol Gomis/UPC, Spain

Industrial supervisor: Dr Peter Heskes/TNO, Netherlands

Session: July 2013

Escola Tècnica Superior d'Enginyeria Industrial de Barcelona
UNIVERSITAT POLITÈCNICA DE CATALUNYA

MSc SELECT is a cooperation between

KTH-Royal Institute of Technology, Sweden | Aalto University, Finland | Universitat Politècnica de Catalunya, Spain | Eindhoven University of Technology, Netherlands | Politecnico di Torino, Italy | AGH University of Science and Technology, Poland | Instituto Superior Técnico, Portugal

Preface

I thank my industrial supervisor Dr Peter Heskes who offered me the chance to do my thesis and initiate the PHIL experiment at TNO. I am grateful for his patience and presence during the course of my thesis, and till the very end. I thank my academic supervisor Dr Oriol Gomis for his kind words and motivation at the beginning of thesis. I would also like to thank him for his prompt guidance during the course of my thesis.

I would like extend a heartfelt thanks to Dr Klaas Visscher for his support for my thesis. It would not have been possible for me to complete my thesis without the support of Jurjen Veldhuizen, TNO; Klaas Bos, Kema; Sjef Cobben, TU/e; Feldbrugge Lude, TNO; Schoolderman Ruurd, TNO Aruba and all colleagues in TNO Eemsgolaan who have my endless gratitude.

My technical background is in energy and power system engineering. TNO offered me a thesis related to ICT and control system, which motivated me to learn new concepts and extend my expertise into new fields. Not only technical knowledge but also project planning skills were acquired during my thesis internship at TNO. I thank TNO for providing this opportunity, financial and technical support to complete my thesis work.

Abstract

Share of distributed generation in grid system is increasing in time. In conventional generation, rotating mass provides inertia to the grid. Distribution generation causes reduction in inertia of grid system and this inertia reduction is one of the challenges that needs to be addressed in the energy transition phase. The number of challenges related to grid stability will proliferate in the future. Research and Development to solve these challenges is ongoing but the developed solutions need to be tested in real time since the performance of new technology in power scale, would be different from mathematical simulation results. Field tests of future grid solution are cost and time intensive while considering construction of a power system. This challenge can be solved by a concept called Power Hardware-in-the-Loop (PHIL). In PHIL, simulated power system can be emulated in real time using power interface. So, new technology can be connected with an emulated power system for testing in power scale.

Since PHIL is an emerging concept, a detailed strategy was formulated for development of PHIL experiment. Frequency Response of a Grid was selected as the focus of power system. In this work frequency response of a power system is emulated in real time using a Real Time System, resistive loads and a power interface with a Motor-Generator set. Triphase interfacing technology is used to interface real time system with hardware. A loop comprising of simulated power system, physical generator and physical resistive load was designed. Real time system and generator mimics emulated power system and the resistive load acted as hardware in the loop. A basic PHIL experiment was successfully completed, in which the change in power of hardware in the loop, affected the emulated power system. Experimental result proves the success of PHIL experiment.

Based on experience and knowledge obtained in a basic PHIL experiment, the conceptual design of a more advanced PHIL experiment of a micro grid that includes virtual power plant is developed. Limitations of the Power Hardware in the Loop experiment is found and reported.

Table of Contents

II. THEORETICAL STUDY

III. DELIVERABLES

1. Introduction

In this chapter, global view of thesis is discussed followed by introduction to concept of Power hardware in the Loop (PHIL). Since PHIL is an emerging technology, section 1.2 has been dedicated to introduce the PHIL concept. In section 1.3 introduction to the Triphase is discussed. The interfacing mechanism for PHIL was enabled by a fast prototyping equipment called Triphase®.

1.1. Global view of this thesis

In this section, relation between PHIL and sustainability is discussed; Power quality issue and motivation of thesis is also discussed.

1.1.1. Contribution to sustainable society

Energy is an important question for human kind. At the end of 20th century human civilisation started to realise the impacts of greenhouse gases on the environment. A major concern rose among everyone in the world. We realised that the major cause for CO_2 emission were fossil based energy resources. Hence we decided to reduce fossil based energy resources. Fossil based energy is primary energy consumption of human society that includes electricity and heating demand. Thus we decided to draw plans for energy transition from fossil based energy to renewable energy resources.

1.1.1.1. Thesis view

Energy Transition aims to reduce CO_2 emission. From appendix A.1, it is evident that Electricity and heat generation sector contribute major portion of CO_2 emission. From global perspective, the thesis is trying to reduce CO_2 emission in electricity sector by developing testing facility that can be used for testing the problems faced during integration of renewable energy into power system.

European society is a forerunner in energy transition thus geographical focus of this report is chosen as Europe.

1.1.2. Need for future grid

AC transmission system won the ‘war of currents’ that happened between Nikola Tesla and Thomas Edison. Thus AC system is being in use for transportation of majority of electrical energy. In other words AC transmission infrastructure is a rigid and proven technical regime for electrical energy transfer. However, it is necessary to rethink the electrical infrastructure due to changes in generation profile as shown in figure 1 and figure 2.

1.1.2.1. Current scenario

Major portion of electricity generation is being dominated by fossil based energy resources. Appendix A.2 proves still Coal, Gas and Oil contribute nearly 50% of total electricity generation.

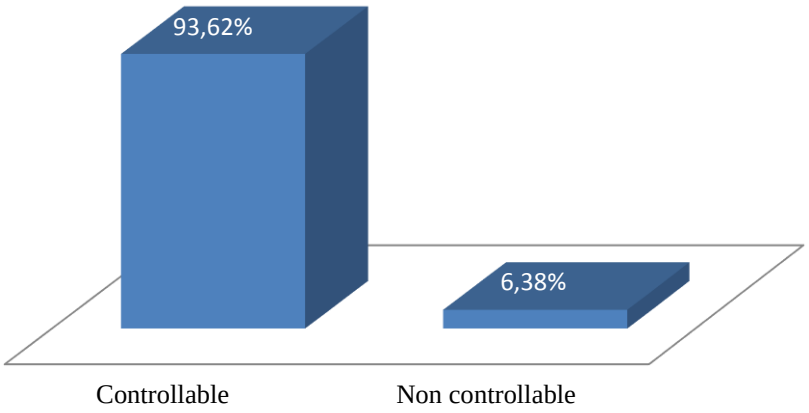

Figure 1 Controllable vs. Non-Controllable power plants on 2009(ENTSO-E)

Comparison between controllable and non-controllable electricity generation resources was made for 2009 shown in figure 1. In controllable generation, power output of plant/unit can be planned and controlled. In non-controllable power generation facilities, power generation cannot be controlled such as solar energy. Thus Coal, Oil, Gas, Hydro, Biofuels and Waste based energy resources are considered as controllable generation facilities. Wind, Solar PV and Solar Thermal considered as non-controllable electricity generation facilities[1]. Figure 1 explains, in 2009 only 6.4% electrical power plants are non-controllable. Thus it is clear that existing aging electrical transmission infrastructure is designed for centralised and controllable power plants.

[1] Nuclear power plants neither considered as controllable or non-controllable power plants. In practice Nuclear power plants act as base load generation units.

1.1.2.2. Future scenario

From figure 2, in 2030, wind and solar based non controllable energy resources will be 17% [17] of total installed capacity. Nature of power generation will be significantly distributed due to roof top Photo voltaic (PV) and micro combine heat and power (CHPs). Current grid infrastructure designed for centralised and controllable generation hence grid infrastructure need to be transformed, so it can handle distributed and non-controllable power generation. Also, it important to realise Electric Vehicles will share a significant portion of load demand. The electrical vehicle charging and discharging can be managed for assuring economic benefits and grid security. Thus it is inevitable that the aging grid system will be modernised.

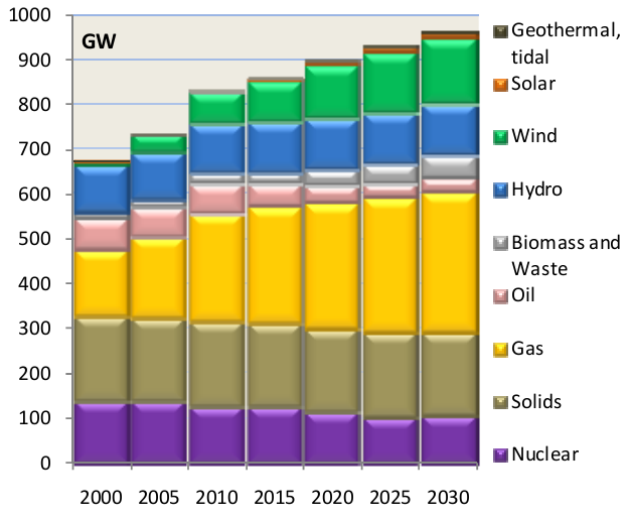

Figure 2 Share of non-controllable generation increases by 2030[17]

1.1.2.2.1 Thesis view

Increasing share of non-controllable generation in the energy mixture demands changes in the conventional electricity grid infrastructure. Needed changes in grid system are being carried out slowly. In practice, change in conventional and proven grid system demands extensive research and development. This research and development is cost and time intensive. To increase the speed and reliability of R&D in modernisation of the electricity grid, a new concept called power hardware in the loop (PHIL) in being developed. This thesis developed basic laboratory PHIL experiment and conceptual design for advance PHIL experiment.

1.1.3. Power quality

Power quality is an important factor in the aspect of grid modernisation. In this thesis, frequency stability of power system is chosen as area of research. Introduction of new power electronics interfaced distributed generation and loads causes number of challenges. More details regarding frequency disturbance are discussed in chapter 2.

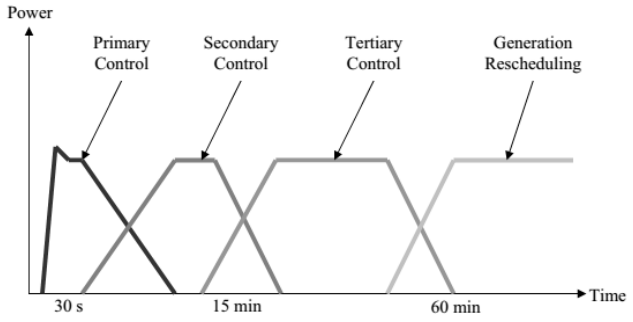

Figure 3 Frequency control and Time scale

As in figure 3, primary control and its impact on grid/grid segment frequency are chosen as focus of this thesis. PHIL experimental environment is used to emulate frequency behaviour of the grid for primary control.

1.1.4. Motivation

In the future micro grids/grid segments and new grid solutions will be developed. Electrical grid parameters are different for different locations for example, zero dead band for primary control in Great Britain. In France tight droop control is emphasized for generator and in Nordic countries for example Norway use of wind farm for frequency stabilisation is analysed. Also, TNO has an international office at Aruba which is an island power system. Behaviour of grid of Aruba is completely different from European scenario. So it is important to develop a platform which can emulate different grid behaviour to test micro grid control algorithms or any other new grid solutions.

There are number of factors that differentiate frequency behaviour of grids from one to other, such as legislation of respective location, availability of reserves, share on non-controllable generation in overall installed capacity, inertia, frequency dependant or self-regulating loads share and network power frequency characteristics of respective grid system.

It is clear that there will be legacy of work need to be done to accomplish advanced PHIL experiment of micro grid laboratory. While considering given tasks and master thesis time frame, following objectives were set for thesis.

- Knowledge generation and development of basic PHIL experiment
- Conceptual design development of micro-grid laboratory

Conceptual design development of micro-grid laboratory is discussed at chapter 5.

1.2. Introduction to PHIL concept

In this section brief introduction to PHIL concept is discussed. Also importance of PHIL for future power system solutions also discussed.

1.2.1. Introduction

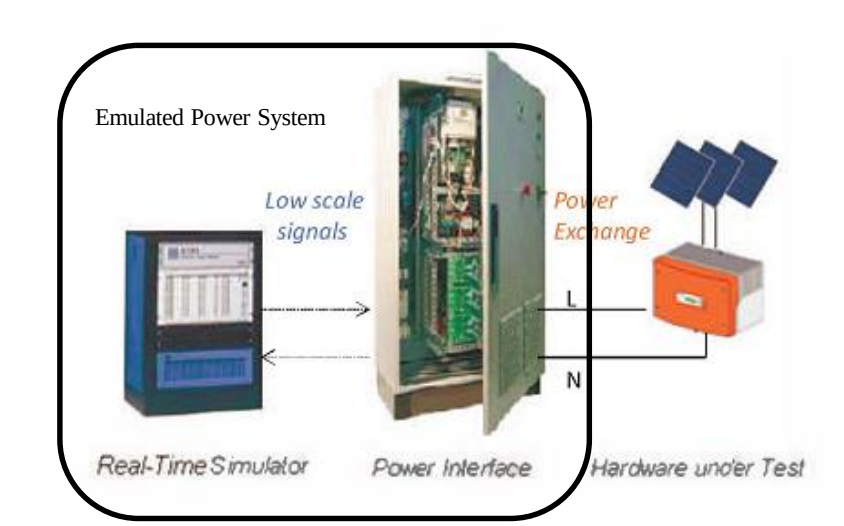

Figure 4 Basic laboratory setup of PHIL [30]

In PHIL experiment, an emulated power system is connected with HUT in power level. Figure 4 depicts that signal output from Real Time Simulator emulated by power interface and HUT is connected with emulated power system. Combination of real time simulator and power interface act as emulated power system. In other words from the PV point of view, PV is connected with real time power system. At the same time, the emulated power system is controlled by a researcher who can simulate different grid scenarios and test the performance of HUT. In conclusion, theoretically the test results of HUT in PHIL environment should show a similar performance of the HUT in the real power system.

Inevitably introduction of hardware in simulation environment leads to new challenges such as time delay, stability and precision of simulation. Experiments in PHIL environment, results in a real time model that interacts with simulation and hardware.

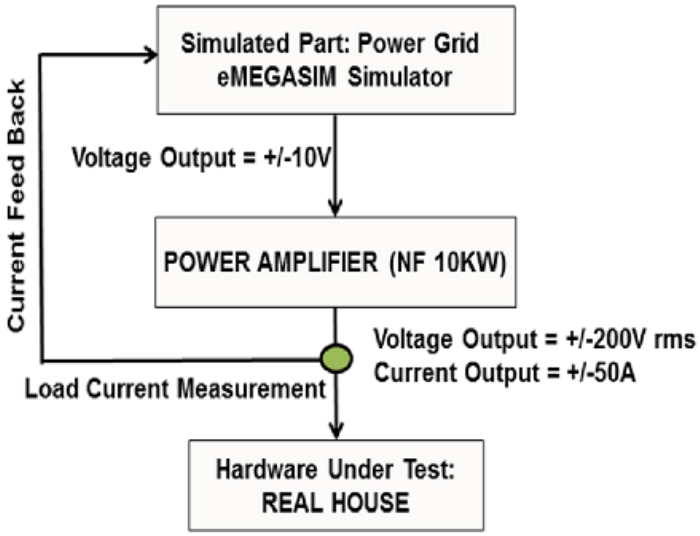

Figure 5 Basic block diagram of PHIL setup [6] (NF=LF)

Figure. 5 is the basic block diagram of working of PHIL setup, in which current is fed back from HUT to RTS by which the performance of HUT can be monitored during different grid scenarios. In experiment by Amine Yamane house current [6] is fed back to the feeder circuit simulated in RTS which returns feeder voltage. It can be noted that an output from physical device drives the emulated power system so the reliability (ability to mimic real time power system) will be higher than numerically simulated power system results.

1.2.2. PHIL in this thesis

Primary frequency response of a grid segment was emulated using a motor generator and real time system. In which physical generator and load were part of a loop that includes simulation model, hence this experiment lies under regime of PHIL and HIL.

In this thesis work, as in figure 5 load current is measured and fed back to real time system. Based on output from real time system frequency performance of motor generator setup is controlled. In this thesis, motor generator setup acts as power amplifier.

1.2.3. Need for PHIL

In process of developing new grid solutions, the test bench to check new solutions are important. A conventional simulation based testing facility is not effective for development of intelligent grid solutions. The reliability of simulation tests depends on availability of accurate models. In PHIL testing, the performance of inverters or distributed generator for different scenarios can be tested in emulated power system.

Before implementing any new grid solutions in real power systems, simulations and lab tests need to be conducted to reduce the risk of failure and to increase reliability of the new solutions. Mathematical simulations can be used to test the new grid solutions. However, availability of accurate mathematical model for PV, wind turbine, fuel cells, grid and loads are limited. In mathematical simulation response of hardware under test (HUT) or new grid solutions, for different environment condition or power system scenarios may not be same as response of HUT in field test. In other words mathematical model may not be able to test the performance of HUT [37] as field test. It leads to a gap between mathematical simulations and field tests [10]. Field test in power system is cost intensive, affects customers [42] and time consuming, so, implementing new grid solutions based on numerical simulations is a risky task. A technique called PHIL is an interesting step to solve this problem.

Power Hardware in the Loop bridges the gap between computer simulation and actual implementation. PHIL is an advanced testing technique compared to mathematical simulations. In a conventional simulation all elements in the simulation are represented by mathematical model. In PHIL/HIL technique, real physical hardware such as PV or Fuel cell will be introduced in the simulation loop. Hence, the performance result of Hardware under Test (HUT) more reliable in PHIL experiments.

Following two techniques can be used to fill the distance between numerical simulation and field test, which are Hardware in the Loop (HIL) and PHIL [10]. After detailed study on HIL and PHIL experiment, comparison between HIL and PHIL was tabled (table1).

Both PHIL and HIL includes real performance of hardware under test (HUT), however most of the distributed generation (DG) are energy generators. Hence, it is better to choose PHIL than HIL which based on signal level. In this thesis work, emulation of power system's frequency response considered as a basic HIL experiment.

Table 1 Comparison of PHIL and HIL experiment

HIL	PHIL
Testing of devices that are connected at signal level with the rest of the system [8], [10].	Testing of devices connected at power and signal level to the rest of the system.
Conservation of energy between simulated network and hardware network is not ensured [29].	Conservation of energy between simulated network and hardware network is ensured.
Mostly used to test secondary power equipment and controllers for machines and converter.	Equipment can connected as they connected in real field.

1.3. Introduction to Triphase- Fast prototyping machine

In this section description of Triphase and its role in PHIL experiment of this thesis work are discussed.

1.3.1. Need for Triphase in PHIL

As shown in figure 4 and figure 5, power interface plays a major role in PHIL experiments. In PHIL experiment, interface between Real Time System (RTS) and hardware will be a challenge. It was found that Triphase® can provide solution for the interfacing problem. On the other hand, Triphase® may be used for future work of micro-grid laboratory setup. Hence current experiment should not be a hindrance for future experiment rather current experiment should act as stepping stone for legacy work of micro-grid laboratory. It was necessary to analyse whole Triphase® setup even though current experiment uses Triphase® for sensors and interface between Hardware and RTS.

1.3.2. Introduction of Triphase

The global view of Triphase is expressed in figure 6. Using Triphase-RTS, inverters supplied by power module of Triphase can be controlled. By controlling the inverters, it is possible to create controllable

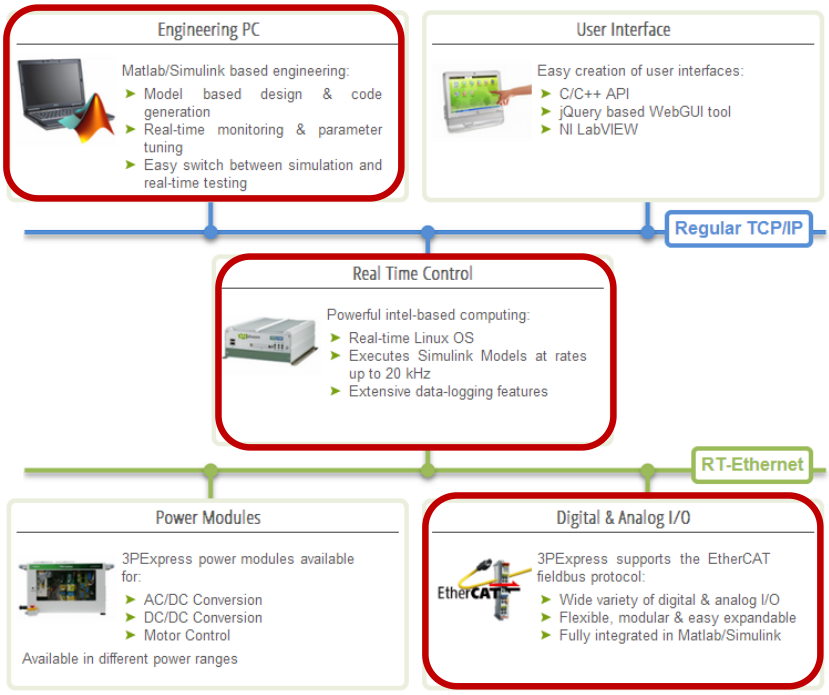

Figure 6 Triphase system overview, reproduced from portal.triphase.eu

power source. Since, power modules of Triphase was not used in this experiment, more details about it described in appendix A.3.

1.3.3. Triphase in PHIL experiment

Triphase® is an electrical equipment which consists of a Linux based computer, sensors, input/output devices (I/O), power inverters and its auxiliary devices. In this thesis, only a part of facilities from Triphase® were used. Though limited facilities from Triphase® were used, control technology of whole Triphase® were studied for development of PHIL experiment.

As in figure 6, facilities from Triphase used in current experiment were highlighted with dark red boxes. In this experiment, Triphase® used as RTS facilitator. The equipment used from Triphase® were listed as follows,

- RTS
- I/O device
- Measurement devices
- Communication architecture

1.3.4. Real time system

Real Time System (RTS) is a Linux based PC power by Intel core 2 duo processor. It acts as the control centre of whole experimental setup. It acquires data and controls I/O devices in real time. It is, ipso facto, the brain of experiment. It interfaces with measurement devices using FPGA.

1.3.5. I/O devices

Beckhoff modules act as the I/O device for Triphase. Beckhoff controls contactors, relay and reads its status. Safety mechanism are monitored and controlled by Beckhoff modules.

1.3.6. Measurement devices

In this experiment three voltage sensors and three current sensors were used. More details of sensors can be found in respective datasheets.

1.3.7. Communication architecture

Communication is an important task in PHIL experiment. PHIL experiment is a real time experiment, Hence data packages are time critical for the success of PHIL experiment. A number of communication facilities were used in the PHIL experiment. In this section, more details about different communication of Triphase are discussed [31]. Figure 7 shows three different layers of Triphase and its significance.

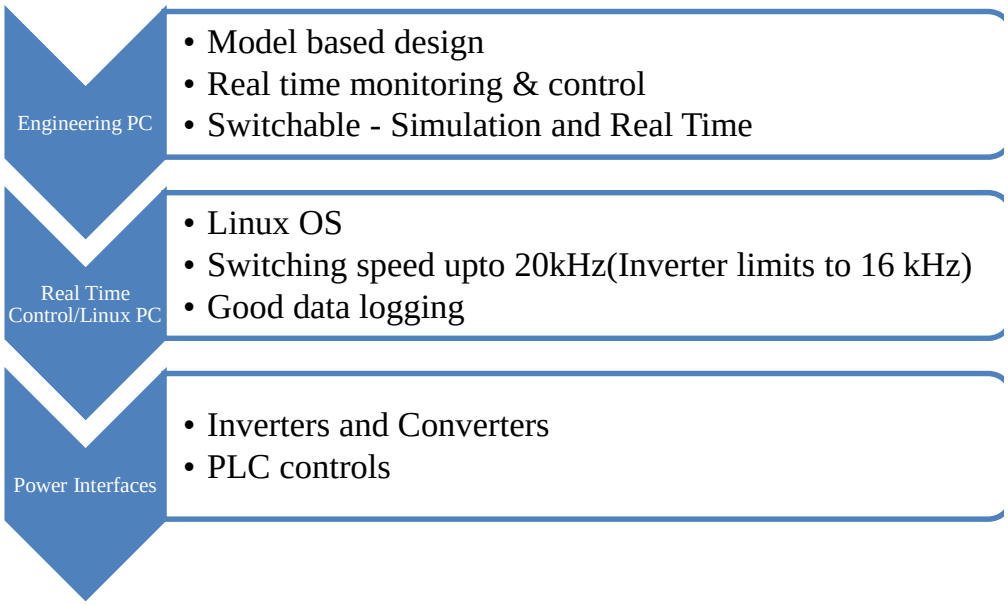

Figure 7 Communication architecture of Triphase

1.3.7.1. TCP/IP

Engineering PC and Linux computer/RTS are connected in regular TCP/IP. Since RTS has TCP/IP connection with Engineering PC, it is possible to connect devices that has TCP/IP with RTS. Once a model is developed in Simulink environment, the model will be verified and code can be generated for real-time execution. The code will be uploaded to RTS through TCP/IP communication link. The typical update frequency for TCP/IP is lies between1-10Hz depends on network load.

1.3.7.2. Ethernet communication

Triphase® has prepared Ethernet protocol for communication between RTS with Beckhoff, I/O and power modules. Ethernet communication speed is denoted in field bus xml file as period_us="50000" micro seconds. XML file of field bus is attached in appendix A.4.

1.3.7.3. Optical fibre communication

There can be many slaves but one master device will be used. The slave devices should synchronise with each other for optimal performance. This synchronisation can't be done with Ethernet communication due to possibilities of delays and line failure. To overcome these problems optical fibre communication is used between two inverters.

1.3.8. Real time system/Linux PC

Linux based PC acts as the central controller in Triphase® setup. All Simulink model will be converted into C code, compiled and executed in RTS PC (Linux PC) - RTS. Power modules, measurement and other I/O devices are communicating with RTS via Ethernet communication. FPGA algorithm is act as interface between RTS and measurement devices and monitors watchdog protocols for overcurrent and overvoltage protection. Figure 8 explains process in every Ts.

1. All measurement data reaches FPGA level at inverter
2. Measurement data sent to RTS via Ethernet commutation
3. Based on measurement data new control signals will be generated at RTS
4. New duty cycle or control signals sent to FPGA level
5. New duty cycles values or control signals implemented for respective devices.

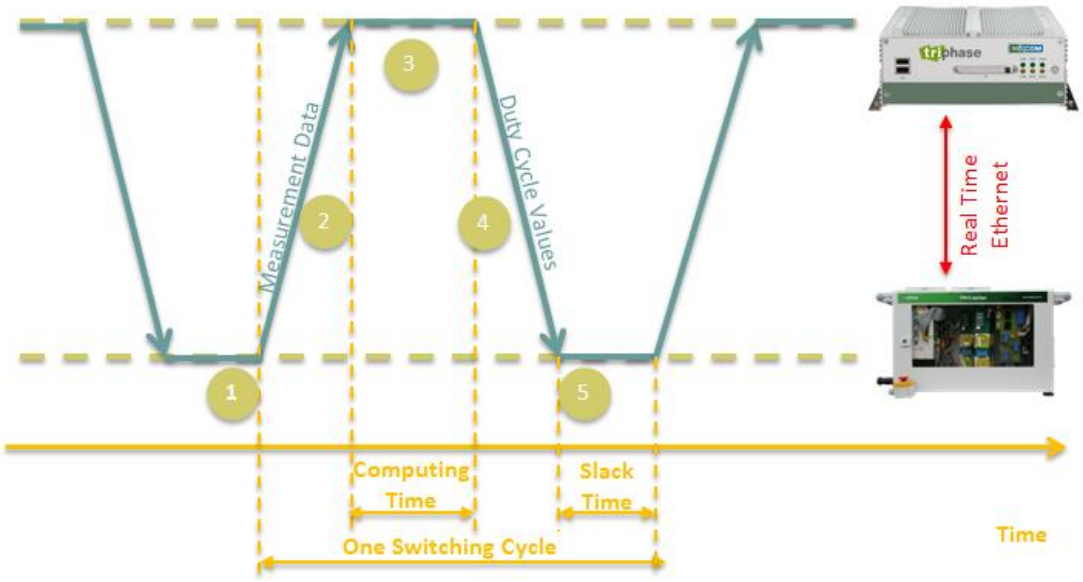

Figure 8 One switching cycle of Real Time Computer [22]

1.3.9. Computing power

Figure 8 is an important concept that determines computing power of RTS. Real Time System needs to acquire data, compute and command interface devices in real time, which needs to be completed within 2Ts. Ts is switching cycle of inverters, which determines the computation time. Switching rate of given inverters varies from 8 kHz-16 kHz. In whole thesis switching time was set as 8 kHz. Simulink model used in this experiment will be discussed in chapter 3. The model needs to be run within 2Ts. The current

model can be computed in 2Ts in other words within 0 latency. For 0 latency the system will have only 2Ts. When model is improved and becomes more complex in future, computer may not have enough computing power to solve the model in 0 latency. TRIPHASE allows to increase[1] latency up to 7. For increase in latency by one the available computation for RTS increases by one cycle. Computational power of RTS limits more complex PHIL experiments. It may be solved by installing RTDS® or OPAL-RT®, which are Real Time Simulators with parallel central processing units. The real time simulators have high computing power and toolbox associated with the simulators will help to develop more complex power system.

[1] Latency value for model can be increased by modifying Triphase system configuration block.

2. Frequency Stability

This chapter dedicated to provide insight in the field chosen for PHIL experiment. In this section frequency disturbance in a power system is being analysed. At the end of chapter, the exact topic chosen for experiment is explained.

2.1. Introduction

Frequency stability is important for power system or maintaining normal operation. The stability of a power system can be perceived in different ways. Stability of power system can be classified as rotor angle stability, voltage stability, midterm and long term stability [27]. In this thesis midterm stability from frequency control point of view remains main objective. Supply-demand imbalance in power system causes frequency disturbance. There are a number of procedures to stabilise the power system after disturbance. Power system operation states is shown in figure 9.

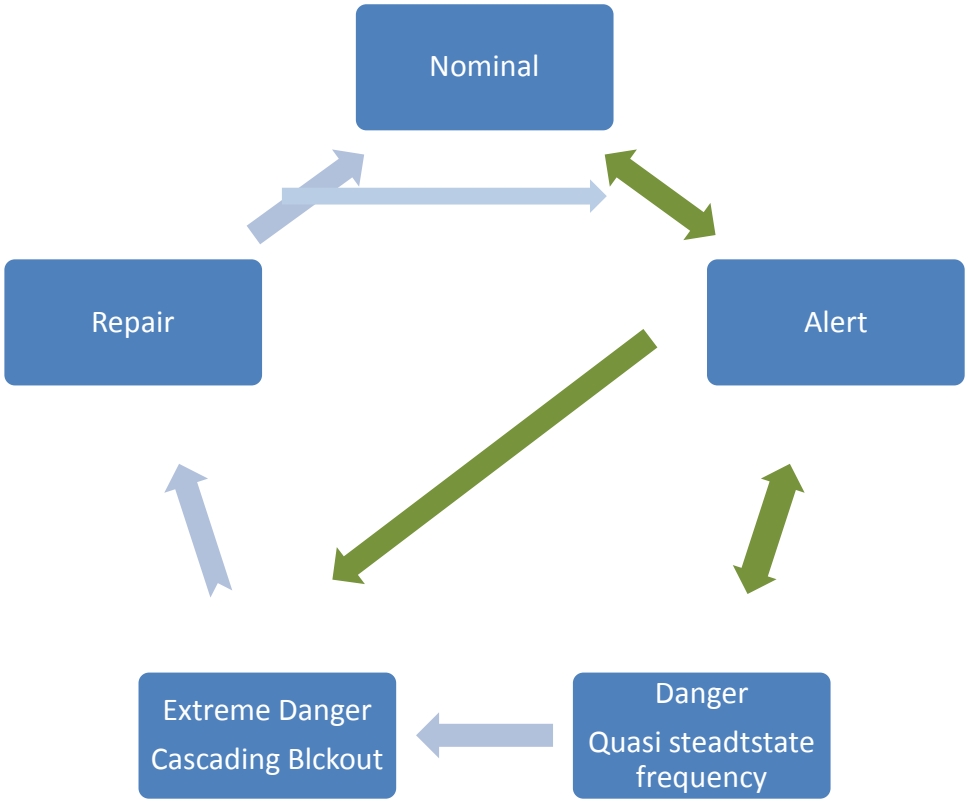

Figure 9 Power system working arrangement [27]

Figure 9 explains the typical operation behaviour of power system. In normal power system, all parameters in the system are in limits. Due to some disturbance and its scale system may enter in to danger or extremely danger situation. In extremely dangerous situation, system will go into cascading load shedding. In danger situation, the system would breach short term limits such as overloading or over voltage. Quasi steady state frequency after primary control activation in the power system, is assumed as Danger situation. If action were not taken in danger situation such as frequency restoration control, system will go to extreme danger situation. In this thesis the transition between Nominal states - Alert state – Danger state is being investigated.

2.2. Different types of frequency control mechanism

As in figure 10 different types of frequency control mechanism were discussed in section 2.2.

Table 2 explains the equivalent names [2] for frequency control in power system. Both names from table 2 are used in report and they represents same meaning. It decided to follow new naming convention of ENTSO-E to convey dynamism in power system operation's and control regime.

Table 2 New naming suggestion from ENTSO-E

Conventional Names	**New Names**
Primary Control	Frequency Containment
Secondary Control	Frequency Restoration
Tertiary Control	Replacement
Primary Control Reserve	Frequency Containment Reserve (FCR)
Secondary Control Reserve	Frequency Restoration Reserve (FRR)
Tertiary Control Reserve	Replacement Reserve (RR)

2.2.1. Primary control or Frequency containment

Frequency containment controls the changes in frequency and maintain system frequency in quasi steady state value. It needs to be activated within 30seconds [12] since frequency disturbance. Frequency containment control depends on many factors including primary control of speed governors, inertia and self-regulating loads. In this thesis, experiment and model are developed for Frequency containment control which are highlighted in green colour in figure 10. For Continental Europe nominal frequency is

set as 50Hz. Maximum quasi steady state frequency deviation is set as 50±0.2 Hz. The maximum dynamic frequency deviation value should not exceed 50±0.8Hz. Controller of primary reserves in continental

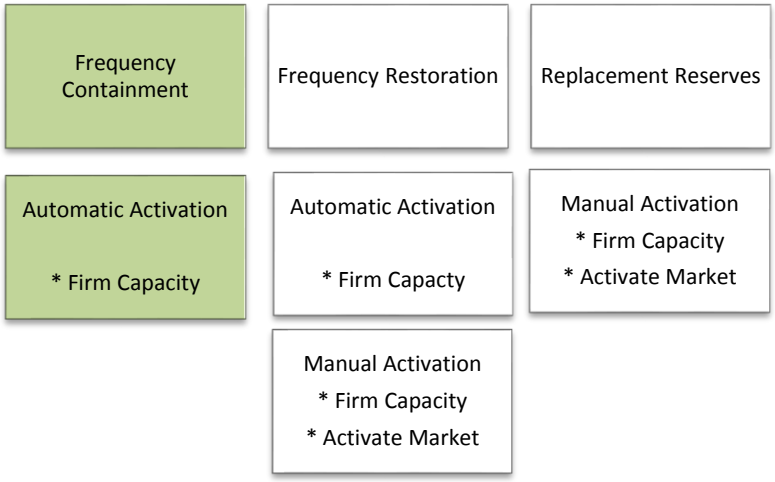

Figure 10 Frequency stabilisation reserves and types

Europe are allowed to have dead band of ±20mHz. More details for other regions such as Baltic, Great Britain, Ireland, Nordic and Cyprus are given in Appendix A (A.5).

2.2.1.1. Inertia

Inertia of a generator is provided by associated kinetic energy of its rotor, shaft and turbine mass. This kinetic energy acts as damping constant that resist change in frequency. In real time, load changes thus introduces supply and demand imbalance. It leads to introduce frequency fluctuation. Since rotating mass rotates at grid frequency, it resists change in frequency.

2.2.1.2. Self-regulating load

Power Consumption of self-regulating load/frequency depend on grid frequency. When grid frequency reduces, power consumption of the load also reduces. This effect helps to maintain supply demand gap. In real time, availability of such loads are reducing due to introduction of power electronics interfaced machines. 1%/Hz of SRL means for a drop of 1Hz overall power consumption will reduce by 1% compare with its nominal power consumption.

Primary Reserves are depend on reference incidents[1] since reference or contingency incident causes maximum expected supply demand gap thus frequency deviation. So reference incidence determines primary reserves.

2.2.2. Primary reserves in smaller grid segment

In a smaller grid segment, number of generators connected with grid would be less. Less number of generators leads to smaller amount of rotating mass and kinetic energy associated with it. Hence it results in lower inertia. Rate of change of frequency will be faster. Dynamic frequency deviation will be higher during events. In smaller grid segments with limited primary reserve and its deployment time, may increase chances for cascading black outs. To avoid such situation in majority of smaller grid segments, load shedding[2] might be used as protective mechanism.

In this section, Aruba was considered as smaller grid segment. Main stream of Aruba's economy is driven by tourism hence load shedding based protective mechanism is not an attractive solution. Load shedding based frequency control mechanism cause inconvenience for tourist which affect Aruba's tourism sector. In this section possibilities of using 30MW of wind farm for frequency stability of Aruba is discussed.

[1] Reference incident determined by ENTSOE. There should be enough reserves available for mitigating problems caused by reference incident. For continental Europe 300MW generation loss considered as reference incident.

[2] It depends on economics of operation and policy of concern government

2.2.3. Aruba - awaiting challenge – a smaller grid segment

Aruba is a small island located 27 km north of the coast of Venezuela (figure 11). It has area of 178.91 km^2. It has tropical wet and dry climate. Average Temperature is mostly around 33 degree Celsius (en.wikipedia.org). Aruba is an island country which clearly explains possibilities quite smaller inertia

Figure 11 Geographical location of Aruba

constant for its grid. Aruba has a vision of Oil free economy. With current electricity market practice and current technology; wind energy and PV constitutes zero inertia constant. Increase of penetration of green energy in Aruba may reduce grid inertia. Aruba may face significant amount of black out during grid disturbances due to lower inertia. Number of solutions, can solve this problem such as artificial sea water pumping storage or micro/macro battery storage or potential wind turbine inertia.

2.2.3.1. Wind energy and its solutions

Wind Energy is not only green energy but also it has some other grid stability solutions. Since thesis only focus on active power imbalance and frequency disturbances in grid system, in this section only active power solutions are discussed. There are two potential grid stability solutions can be exploited from wind farm, which are

- Wind turbine inertia
- Active power control/frequency restoration reserve using pitch

It is explicit, both control technologies can be used only when wind energy is available. Whenever wind energy is available and decided to consume it, another fossil based generator unit (controllable generator unit) will be disconnected from grid. The disconnection causes loss of inertia and primary reserve contributed by the disconnected generator.

2.2.3.2. Frequency restoration reserve

The wind turbine can operate lower than its optimal point. In this case whenever load increases or loss of transmission line of generator can be compensated by increasing performance point of wind energy. Possibilities of this technology is explained with help of figure 12 and figure 13.

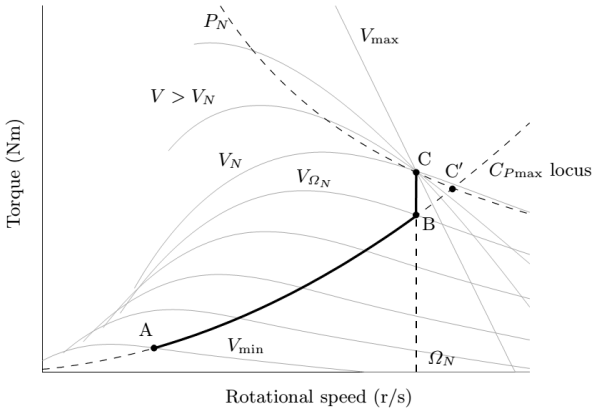

Figure 12 Basic variable speed, variable pitch wind turbine control [19]

Since the complete control strategy is out of scope of this thesis, only required information is discussed here. Figure 12 explains operational points of variable speed variable pitch wind turbine. This type of wind turbines are capable of producing maximum possible power for different wind speed. As in figure 12, normally wind turbine follows C_{Pmax} locus curve. If we can control C_{Pmax} locus curve power extraction

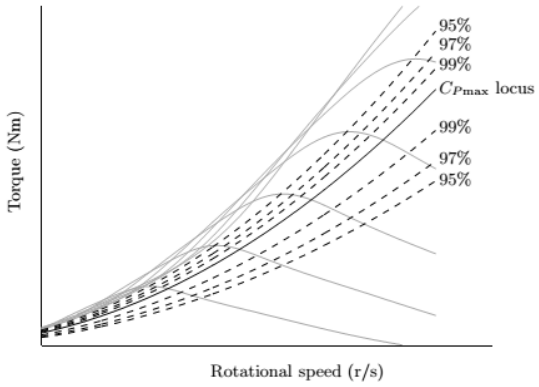

Figure 13 Different Cp curves [19]

from wind turbine also can be controlled. It gives possibility of control of active power output from wind farm like conventional power generation units. Possibilities of controlling C_{Pmax} locus curve is proven with following figure 13.

Figure 13 is the Cp controller behaviour of wind turbine during turbulence. By controlling pitch angle of wind turbine, C_{Pmax} locus curve can be controlled. Wind turbines in Aruba has pitch control. Figure 13 proves wind turbine can operate at 95% of optimal point by controlling pitch in all wind speed. It is possible to operate wind turbine always at lower optimal point, like mandatory 3% rated power reserved for primary control in controllable generator unit. Whenever grid needs active power support (lower frequency) C_{Pmax} locus curve can be improved to 100% and provide support to grid. However, this control strategy causes loss of annual energy generation. Hence more economical study should be made before implementing this control. Also deployment time of this active power is limited by the speed of pitch activating motors. This concept can be a solution for Aruba grid problem. However, this concept is not implemented in HIL environment.

2.2.3.3. Inertia – opportunity of wind turbines

$$H = \frac{stored\ ennergy\ in\ rated\ speed\ in\ MW.s}{MVA\ rating} \tag{2.1}$$

$$Stored\ Enenrgy = \frac{1}{2} * J * \omega_{0m}^2\ W.s \tag{2.2}$$

$$\omega_{0m} = 2\pi \frac{RPM}{60}\ rad/s \tag{2.3}$$

In Aruba, 10 number of Vestas V90-3.0 MW wind turbines were installed [1]. In nominal operation V90 has rpm of 16.1 [43] and ω_{0m} is 1.686 rad/s. Moment of inertia of generic model of 3 MW wind turbine is 12.6e6 kgm^2 [25]. By applying these values into equation 2.2,

Stored Energy in one V90-3.0MW at nominal operation = 17.898 MW.s

Total stored energy from wind farm is 178.98 MW.s.

Average demand of Aruba is 103 MW and peak demand reach up to 125MW [44].

Since transformer ratings are not available, it is assumed that transformer in Aruba has infinite rating and capable transferring any amount of power from wind farms. Also power factor is assumed to be one. For average demand, Inertia constant value for wind farm is calculated as

$$H = \frac{103}{178.98} = 1.74\ s$$

Due to addition of wind turbine inertia into grid system, Aruba grid inertia constant can be increased by 1.74 s from current inertia constant for average demand. During peak demand inertia constant can be increased by 1.43 s.

2.2.3.4. Summary of Aruba wind farm inertia constant

In this section, the potential opportunity of using Aruba wind farm's rotor inertia as frequency containment reserve is discussed. The existing Vader Piet, Aruba wind farm is capable of increasing inertia constant of Aruba grid system by ~1.5 seconds. Hypothetically, though all power generation facilities in Aruba are failed, Vader Piet wind farm alone can provide electricity to Aruba for 1.43 seconds.

In Aruba as penetration of renewable energy and demand increases, the frequency containment and frequency restoration reserves will be expensive. Thus economic feasibility of operating wind farm in lower maximum power point is an interesting concept; it is recommended to conduct more research in this field.

2.3. Secondary control / Frequency restoration

Secondary control uses secondary reserves to bring back frequency from quasi steady state value to nominal value. It is being implemented by controlling new set value for contracted generator. Secondary control should be activated in 30 seconds to free FCR. Since frequency disturbance is global event across control areas all generators in synchronous area will be at quasi steady state frequency thus causes supply-demand imbalances among control areas. This event result in un-programmed energy exchange between control areas. This effect need to be eliminated within 15mins by control area [14], which initiated primary control. Only affected control area/TSO implements secondary control provided it has contract with another control Area/TSO for secondary control reserves. FRR is automated and market based in continental Europe however it is manual control in Nordic countries [2]. The secondary control is market based it can be Marginal Pricing Mechanism or Pay as Bid mechanism. The secondary control area error estimation is based on many factor including calculated risk however thesis focussed on primary control. Hence more details regarding secondary control is not discussed in this thesis.

2.4. Tertiary control

Tertiary Control Reserve will replace Secondary Control reserve for next event. Tertiary control ensures availability of secondary control for next disturbance and/or redistribute secondary control to various generators in cost effective way. It usually accomplished by shutting down of generator unit or pumped storage or rescheduling interconnectors program [15]. Figure 14 explains time of operation different kind of reserves which maintains system frequency.

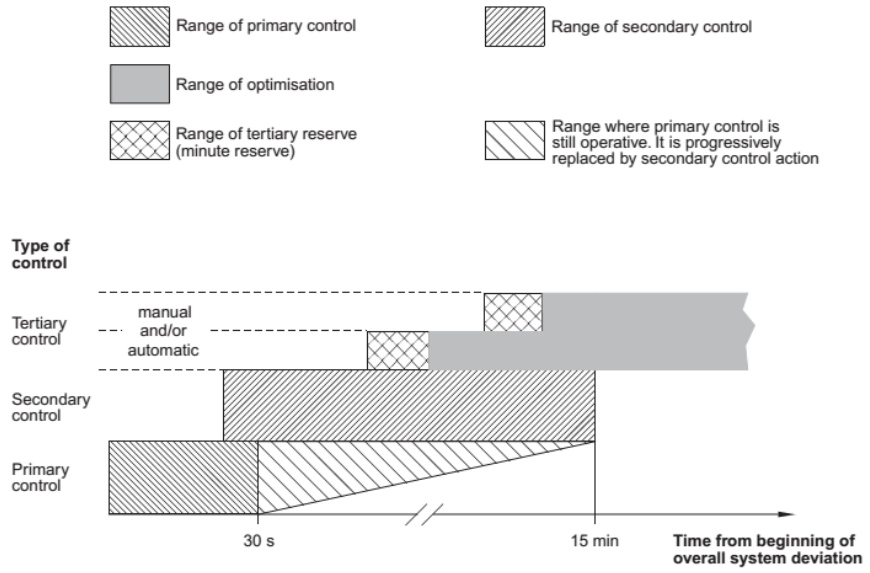

Figure 14 Difference reserves and its time criticalness [14]

2.5. Frequency dynamism in different grid architecture

When considering generator connected to a big and integrated grid system (infinitive bus). Changes in grid frequency affects output power of generator. Droop Control characteristics of generator will force the generator to produce power for new grid frequency.

When considering island operation and assuming generator output voltage is constant. Generator output power is set for 50/60Hz and for constant load. Whenever there is supply demand balance disturbed change generator droop control will force system to operate in new frequency. The whole grid will be in the new frequency. This concept is used to mimic operation of grid segment. It is possible to mimic primary control behaviour of grid segment by finding network power frequency of grid and simulating

FCR deployment time. This approach was followed in modelling to emulate grid frequency behaviour more details can be find in chapter 3.

2.6. Role of TSO and DSOs

At Liberalised electricity market, TSO remains for frequency stabilisation. TSO needs to follow ENTSO-E legislations. TSO will establish contracts with energy produces to comply with ENTSO-E regulation for frequency control. DSO has no role in frequency management of grid.

Because of fast growing distributed energy generation, DSO can exploit the potential of virtual power plant (VPP) thus establish contract with TSO for frequency control. More details regarding this is provided in chapter 5.

2.7. Real time frequency disturbance

The efficiency model was proved by recreating 04 Nov 2006 grid disturbance. More details about it can be found in section 4.4.3.

There can be major frequency disturbance in grid system due to many reason such as natural disaster or significant amount of generation/ transmission line loss or human errors. Figure 15 is such an event in which frequency almost reached 49 Hz. This event caused by improper contingency planning of north Germany TSO on 04 Nov 2006. Cause of this event is not explained here since it does not comes under objective of thesis. In this thesis the event was tried to recreate. During this event UCTE system divided into three areas as in figure 16.

Though quite high frequency disturbances is quite rare however the event on 04 Nov 2006 proved there

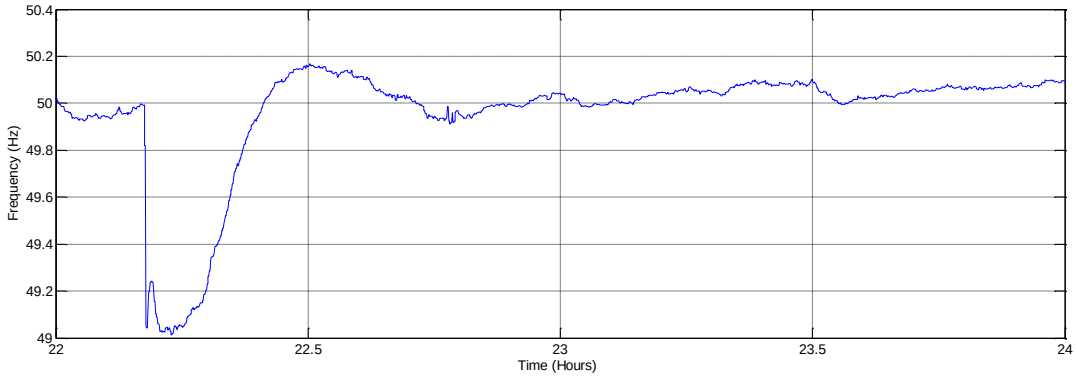

Figure 15 Frequency disturbance on 04 Nov 2006 (source. TenneT)

is possibility of higher frequency disturbances. So there should be sufficient measures taken to avoid this kind of disturbances. All control area in the synchronous are severely affected [13].

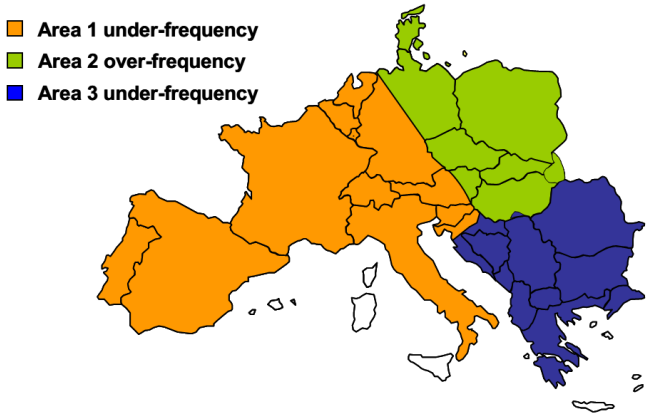

Figure 16 Grid splitting on 04 Nov 2006 frequency disturbance [41]

At the same time, in era of decentralised power generation possibilities of self-sustained power societies are being realised in slow manner. In this case, the upcoming micro-grid can immune itself from such frequency disturbance.

The thesis is trying to emulate such incident that includes flexibility of inertia constant, self-regulating load and network power frequency characteristics.

3. Simulation Model

In this chapter process followed for developing PHIL experiment is discussed. Also, simulation model for emulating primary frequency behaviour of a grid segment is being discussed in detail.

3.1. Development of PHIL

Thesis aimed to accomplish a basic power hardware in the loop experiment. As explained in section 1.2, it was decided to mimic primary frequency behaviour of grid segment in PHIL environment.

Since PHIL experiment is an emerging technique within TNO, a strategy was developed to complete experimental setup for PHIL experiment. Figure 17 explains each steps involved in the strategy of PHIL laboratory experiment development.

3.1.1. Basic requirement

The experiments need to be done in a laboratory called Renqi located in Groningen, the Netherlands. B-VCA (safety course) is entry requirement for working in the Renqi laboratory. B-VCA exam was successfully completed and license was obtained. The scanned certificate attached in appendix A.6.

Installation of Triphase® Toolbox and tutorial for operation of Triphase were studied. More details regarding Triphase® can be found in section 1.3 and appendix A.3.

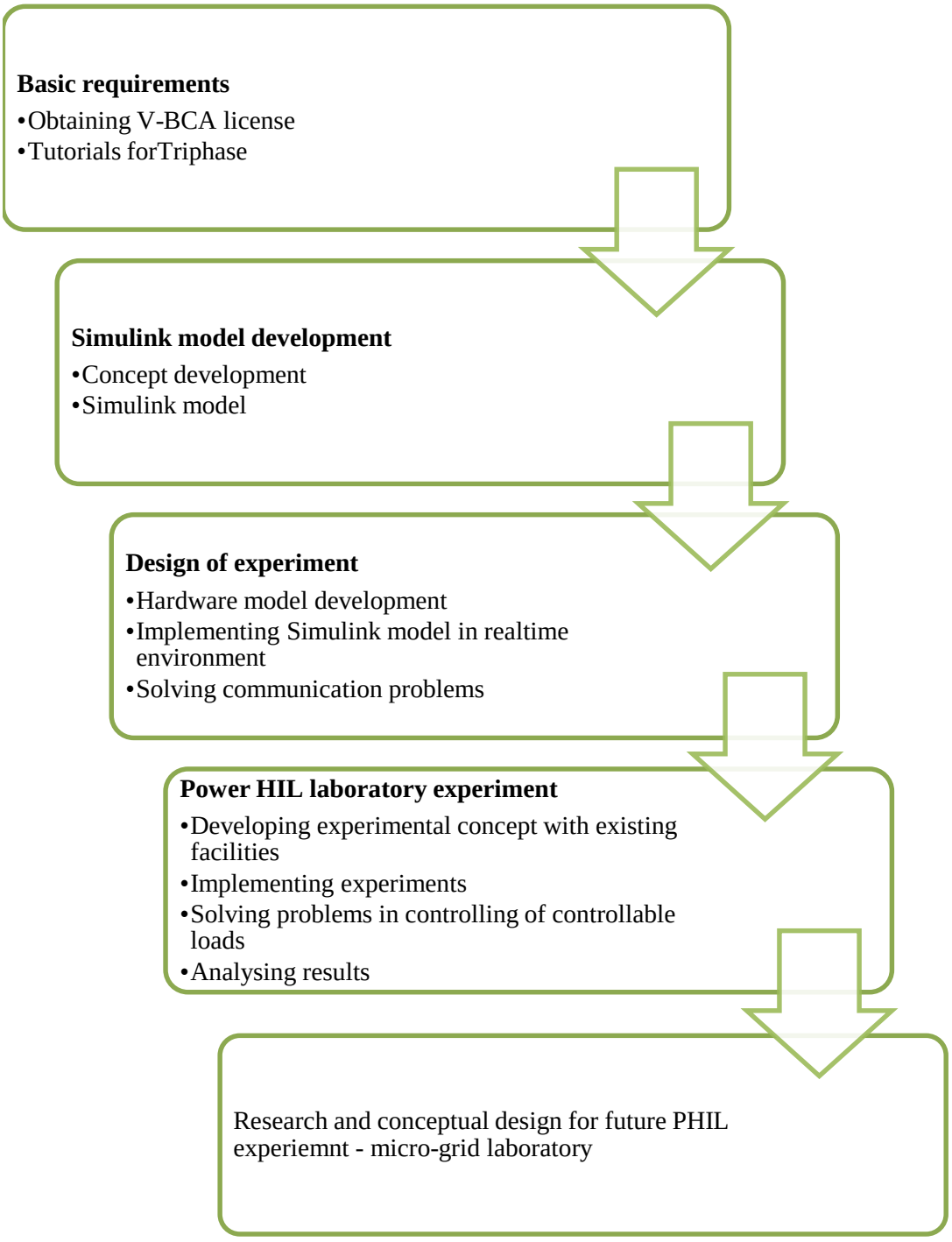

Figure 17 Strategy of PHIL experiment development

3.2. Modelling

In this section modelling of inertia, self-regulating load, network power frequency characteristics and primary reserve deployment time are being discussed.

3.2.1. Simulink model development

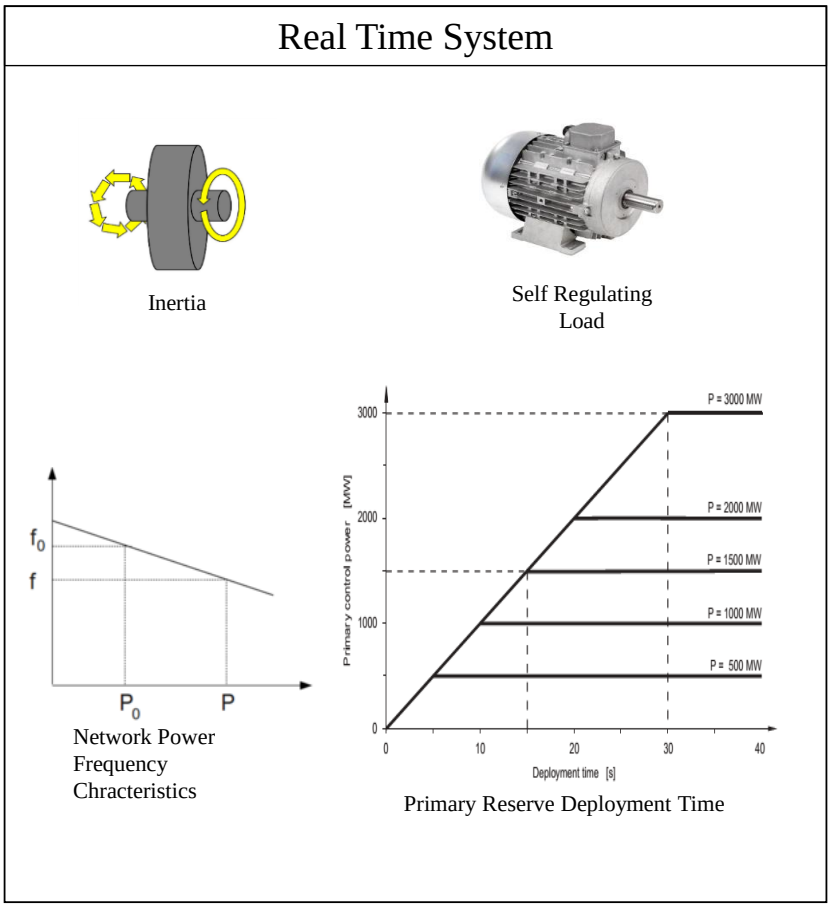

Figure 18 Graphical illustration of real time model

Simulink model was developed to simulate the concepts shown in figure 18 in real time. The procedure followed for the model development is explained in this section.

3.2.1.1. Assumptions

Simulink model was developed based on following assumptions

- Reactive power flow is neglected.

- Ideal Automatic Voltage Regulator is assumed thus irrespective of load/generation changes Voltage will remain constant. Thus change in frequency only depends on active power flow.
- Transmission loss considered to be zero thus load is equal to generation.
- Frequency stability analysed from one second to couple of seconds thus rotor angle stability is not considered for this thesis, which is in range of ms [21].
- Dead zone in droop control is not considered.
- The supply demand gap (input) of model is resultant of generators and transmission lines models.
- Simulink model is developed for simulating primary control[1] effect on grid segment hence simulation result has high accuracy for first 30 s since disturbance. Simulation result's accuracy reduces after 30 s since the disturbance.

3.2.2. Inertia derivation

Derivation for relationship between frequency and inertia was already derived; which is being reproduced for Simulink model.

Swing equation expresses dynamic behaviour of generator i; m stands for mechanical related parameter and e stands for electrical related parameters. More details about this derivation can be found in [7].

$$\dot{\omega}_i = \frac{\omega_o}{2H_i}(T_{mi(p.u.)} - T_{ei(p.u.)}) \tag{3.1}$$

$\dot{\omega}_i$ Stands for angular frequency of generator i. Pre disturbance frequency is denoted by $\omega_i(t_0) = \omega_0$.

In frequency variation point of view equation 3.2 is interesting

$$\Delta\omega_i = \omega_i - \omega_0 \tag{3.2}$$

It is important to note that$\Delta\omega(t_0) = 0$, in other words predisturbance condition.

Equation 3.1 in power values can be written as 3.3

$$\Delta\dot{\omega}_i = \frac{{\omega_0}^2}{2H_i\omega_i}(P_{mi(p.u.)} - P_{ei(p.u.)}) \tag{3.3}$$

[1] Primary control need to be operated within 30 s since the disturbance

Equation 3.3 in actual values can be written as equation 3.4

$$\frac{2H_i S_{Bi}}{w_0}\Delta\dot{\omega}_i = \frac{\omega_0}{\omega_i}(P_{mi} - P_{ei}) \tag{3.4}$$

As the experiment try to simulate a grid/ a segment of grid which contains n number of generators, those generators connected to same bus such that presents centre of inertia of system. In simple terms, it is considered as one single unit. So equation 4.4 for n number of generators can be written as 3.5

$$2\sum_{i=1}^{n} H_i S_{Bi}\frac{1}{\omega_0}\Delta\dot{\omega}_i = \sum_{i=1}^{n}\frac{\omega_0}{\omega_i}(P_{mi} - P_{ei}) \tag{3.5}$$

By considering all individual generator as single unit equation 3.6 can be achieved

$$\Delta\dot{\omega} = \frac{\omega_0^2}{2HS_B}(P_m - P_e) \tag{3.6}$$

For obtaining linear equation of 3.7 it is assumed $w = w_0$ and it is true that $\dot{w} = 2\pi\dot{f}_0$

$$\Delta\dot{f} = \frac{f_0}{2HS_B}(P_m - P_e) \tag{3.7}$$

Following assumption are made for obtaining more useful equation

$$P_m = P_{m0} + \Delta P_m$$

$$P_e = P_{e0} + \Delta P_{load} + \Delta P_{loss}$$

$$\Delta P_{loss} = 0$$

With these assumption equation 3.7 can be written as 3.8

$$\Delta\dot{f} = \frac{f_0}{2HS_B}(\Delta P_m - \Delta P_{load}) \tag{3.8}$$

Equation 3.7 is implemented in Simulink environment and the implementation can be seen in figure 19

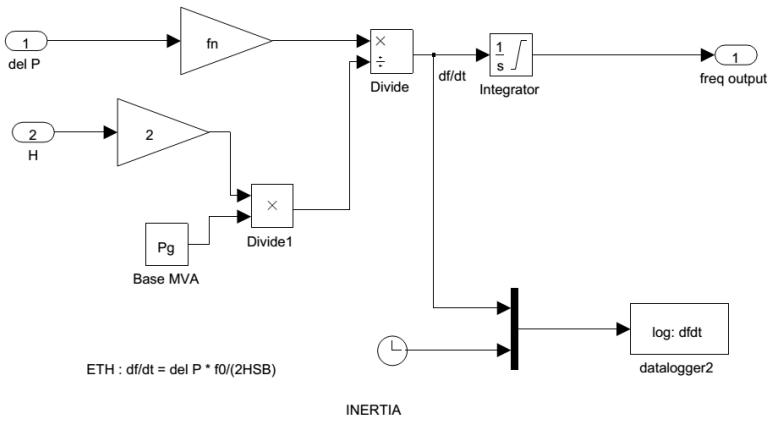

Figure 19 Simulink model of inertia simulation

3.2.2.1. Simulation case 1 for H modelling

It was assumed generator with capacity of 26.559GW and inertia constant as 7 s. In this hypothetical case, the system can provide rated power of 26.559 GW for 7 s even without any input to generator [4].

Figure 20 is the result of hypothetical case developed based of assumption in table 3. As explained earlier

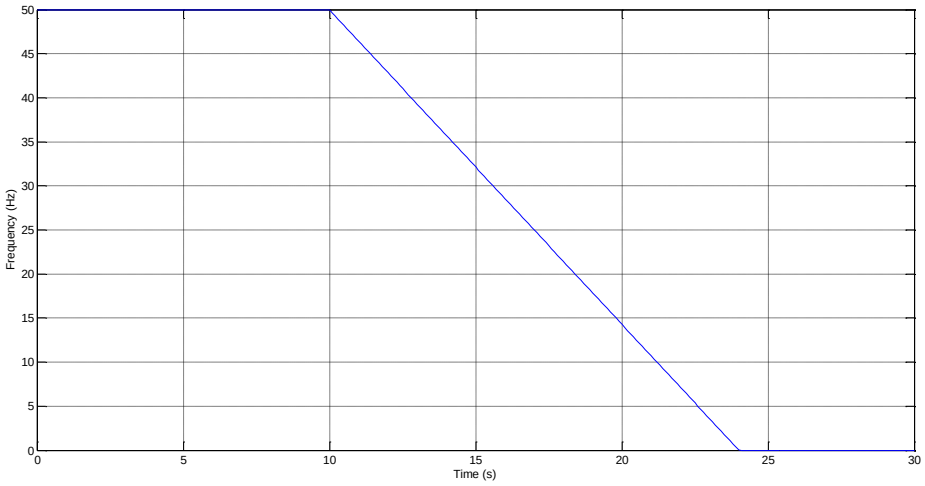

Figure 20 Impact of H on system

when disturbance occur in a system, balance between supply demands varies. In this example the system without primary control is considered. Hence, if disturbance occurs there will not be any change in generator output thus change in frequency will continue. In practice if frequency exceed limits over/under frequency relays trips. But in this hypothetical case, there was no frequency control protection mechanism and self-regulating load. Imbalance between supply and demand is 50% nominal capacity of generator

and H is assumed as 7sec. Figure 20 shows that frequency took 14 sec to reach zero, until frequency reaches zero it can supply load power.

Table 3 Assumptions for H test

Variable	Value	Unit
Nominal Rating	26.559	GW
Imbalance Time(Load)	10	s
Imbalance Load	13.2795	GW

3.2.2.2. Simulation case 2 for H modelling

No primary control is assumed but two various inertia constant assumed that are 2 and 4 respectively and its impact on simulation also noticed. From figure 21, while H increases slope of the system reduces since higher the inertia cause higher resistance to change of frequency. This case proves presence of inertia in the system.

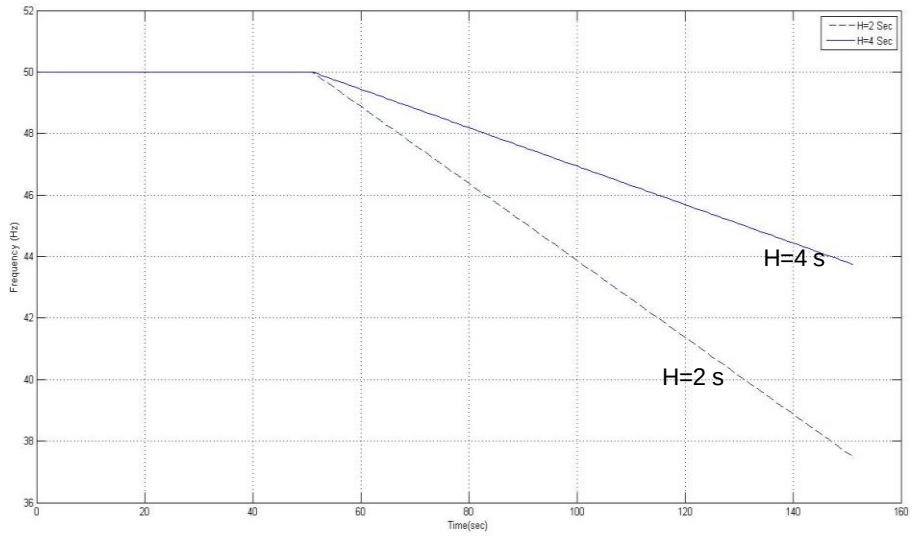

Figure 21 Absence of primary control but inertia presence

3.2.2.3. H value for EU Grid

In this section inertia constant H for continental European Union (EU) grid was analysed. Equation 3.9 is the equation for Inertia constant 'H' [33].

$$H_{gen} = \frac{\frac{J_{gen}}{p^2} {w_{el,0}}^2}{2S_{gen}} \tag{3.9}$$

J_{gen} is inertia of generator in kgm^2 $\omega_{el,0}$ is elelctrical angular velocity at initial/pre disturbance condition. S_{gen} stands for rating of the machine. Considering European Grid as a one generator unit equation 3.9 used to calculate H value for EU grid with following assumption EU generator is two pole machine and rating as 800GW. Number of pole pairs (p) assumed as one. J value found as 1.1e8 [21].

H vale for EU grid is found as 6.784 s.

3.2.3. Primary control

Primary Control is implemented in two ways

1. Using Network Power Frequency Characteristics for grid segment
2. Using Droop constant for generators

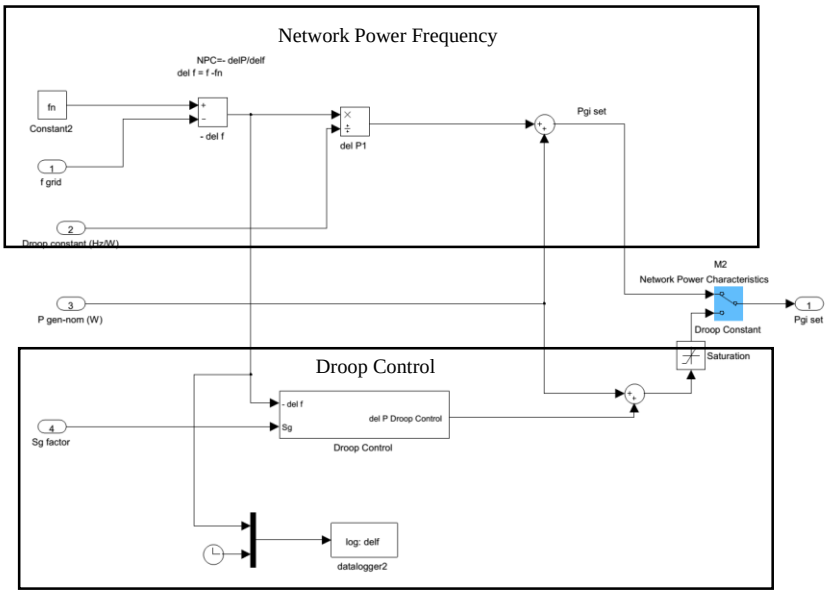

Figure 22 Simulink model of droop and network power frequency control

Primary control of a system/generator safeguard system from being collapsed. The behaviour of primary control is simulated in two mechanism. It is important to note that primary control will help system to reach quasi steady state. However, secondary control is necessary to bring back system to its nominal value. The thesis only focus on primary control and its implementation in PHIL environment.

Figure 22 shows the simulation model of droop control and network power frequency characteristics. More details regarding this as follows.

3.2.3.1. Primary control by droop control

Droop control in a generator is being obtained by governor speed control mechanism. When grid frequency varies from its nominal value. Generator output will vary based on droop constant of it. It can be observed from figure 23, due to loss in load frequency of system increases, to compensate the disturbance the generator needs to reduce its active power output. The change in output power being done by primary controller/speed governor of generator. Primary reserves needs to be deployed before 30 s.

Figure 23 is simulation result of primary control that has following assumption. Generator rated power is 100MW and 1% rated power is reserved for primary control. For smaller frequency disturbance, generator with 4% droop constant participate more to mitigate frequency disturbance than generator with 40% droop. At the same time generator B responds to frequency disturbance in the range on 49.8 and 50.2 Hz. So participation of generator for frequency disturbance is being determined by droop control constant.

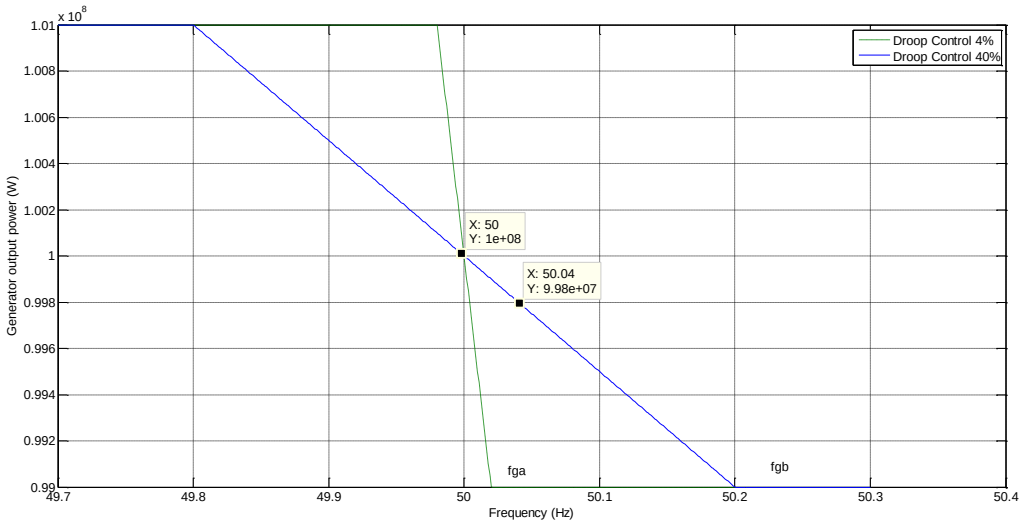

Figure 23 Primary control of generators with different droop constant

Testing of droop constant based primary control

For this hypothetical simulation generator's rated power assumed as 100MW, droop constant assumed to be 4% and infinite amount of primary reserve also assumed. If droop control is 4%, speed governor will direct generator to produce 100% rated power for frequency change of 4%; in this case frequency change of 2Hz causes 100% change in power output [27]. This effect can be seen in figure 24. This test proves ability of droop control of model.

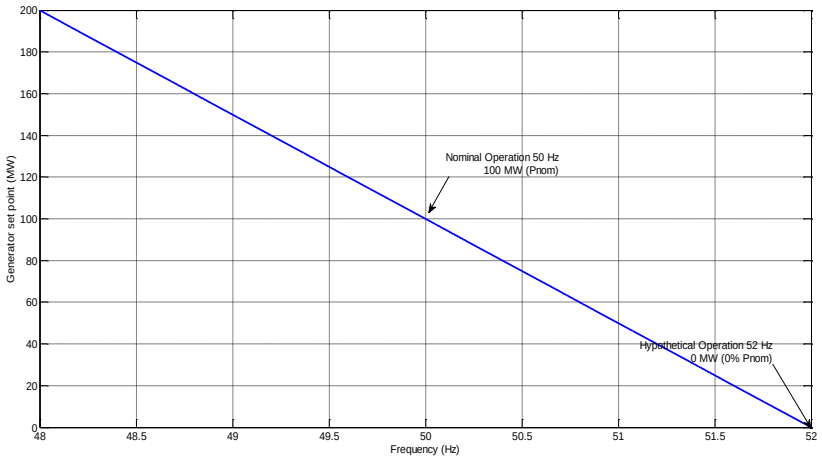

Figure 24 Testing of droop constant based primary control

Summary

Droop control of an individual generator simulated successfully. However, thesis focus on grid segment this model was not used for PHIL experiments.

3.2.3.2. Primary control by network power frequency (λ) characteristics

In this thesis for PHIL experiment, Network power frequency characteristics based frequency control was used. Since λ represents primary control of a grid segment.

$$\lambda = \frac{-\Delta P}{\Delta f} \left(\frac{W}{Hz}\right) \tag{3.10}$$

Network Power frequency is a measure that relates power deviation and frequency deviation after a disturbance for a given grid system. Equation 3.10 is mathematical representation of λ. This concept is used in model, to simulate primary frequency behaviour of a grid segment. In a grid segment, number of generator with different droop constant and different primary reserve would be connected. Modelling different kind of generator and its turbine are out of scope of this thesis. Hence, to simulate grid segment λ is used. Network power frequency characteristics creates a linear relation between frequency of grid segment and cumulative generation power of generators in the grid segment. It can be observed from Figure 25. Figure 25 is the result of system with 300GW network power in nominal condition and λ value as 1800MW/Hz [14] . For 50 Hz nominal operation, power generation of grid segment is 300 GW. Hypothetically considering load increased by 18 GW. Load increase caused supply-demand gap of 18GW.

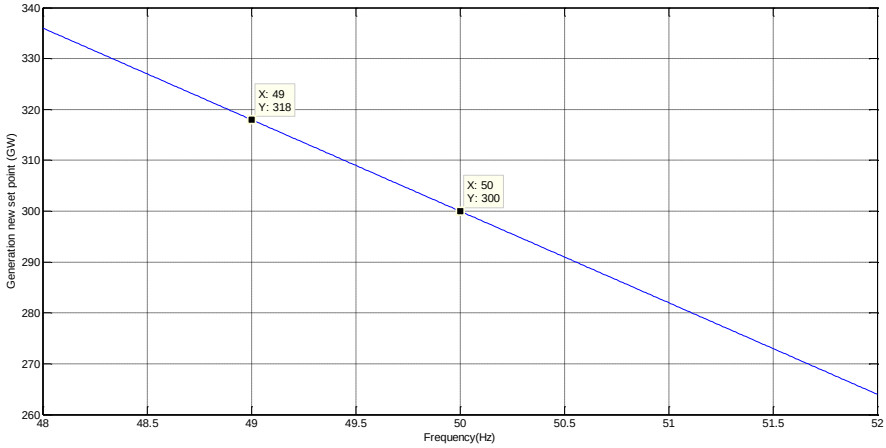

Figure 25 Network power frequency simulation result

Due to supply demand gap, grid segment frequency reduces. Frequency reduction stopped at 49 Hz in the grid segment. Because, all generators in the grid segment did increase their output power[1] and it continues until cumulative power generation of the grid segment is increased to 318 GW.

[1] Because of droop setting output power of generation varies with grid frequency. Droop setting determined by energy supplier and TSO based on network power frequency characteristics of area and contract between them.

In conclusion, Network power frequency characteristics represents cumulative droop constant of generator in the control area.

3.2.3.2.1 Network power frequency characteristics of the Netherlands

For a grid segment primary control and self-regulating load can be represented by Network Power Frequency Characteristic (λ_i). Equation 3.11 denotes λ of i^{th} control area.

$$\lambda_i = C_i \lambda_{syo} \tag{3.11}$$

Ci is contribution coefficient of control area of i. λ_{syo} is power frequency characteristic of whole synchronous area.

λ_{syo} is calculated using equation 3.12 which is ratio between load change and respective frequency change.

$$\lambda_{syo} = \frac{-\Delta P}{\Delta f} \left(\frac{W}{Hz}\right) \tag{3.12}$$

Netherlands is a member of continental European continental synchronous area λ_{syo} for continental Europe is found as -15 (GW/Hz) by taking ENTSO-E assumption as follow ΔP as 3000MW and Δf as 200mHz and λ_{syo} for Europe while including self-regulating load is 16.7 (GW/Hz).

Using equation 3.13 Contribution coefficient for Netherlands is found

$$C_i = \frac{\sum Energy_i}{\sum Energy_{sy}} \tag{3.13}$$

$\sum Energy_i$ is generation of Netherlands on 2011 including exports $\sum Energy_{sy}$ is generation of continental Europe synchronous area on 2011. The values of these value found from [11] and Data provided by ENTSO-E.

In conclusion, Ni or λ for Netherlands was found as 623.63 (MW/Hz) and including self-regulating load it was 692.92(MW/Hz).

3.2.3.3. Difference between network power frequency characteristics and droop primary control

Theoretically the operation principle of network power frequency characteristics and droop control are similar. In this model both concepts were modelled to improve flexibility and user friendliness of model.

Network power frequency characteristics constant can include effect of self-regulating load but droop constant cannot include effect of SRL.

3.2.3.4. Primary control dynamism

Primary Control in a generator will not respond instantaneously, there will be some delay due to mechanical constrains of turbine. The delay time for primary reserve deployment varies from generator to generator. In case of Gas generator response would be faster than coal generator. However, ENTSO-E regulates response time of primary control within 30sec.

Main purpose of the model is to simulate grid segment. In case of grid segment, for primary control reserve deployment time ENTSO- E have regulation; that are primary reserve should be available within 30sec and 50% of primary reserve should be available within 15sec.

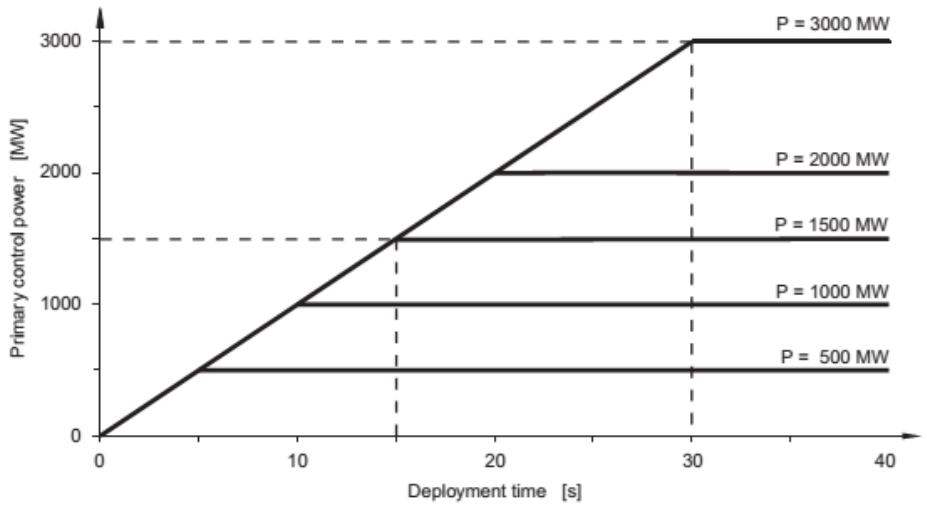

Figure 26 Primary control response time [14]

Figure 26 is picture reproduced from ENTSO-E report that shows the dynamism of primary control in a grid segment. First order system with time constant of 5 s is used to simulate primary control response behaviour. Figure 27 is the Simulink model of primary reserve deployment time dynamism. Figure 28, shows the simulated behaviour of primary control in model.

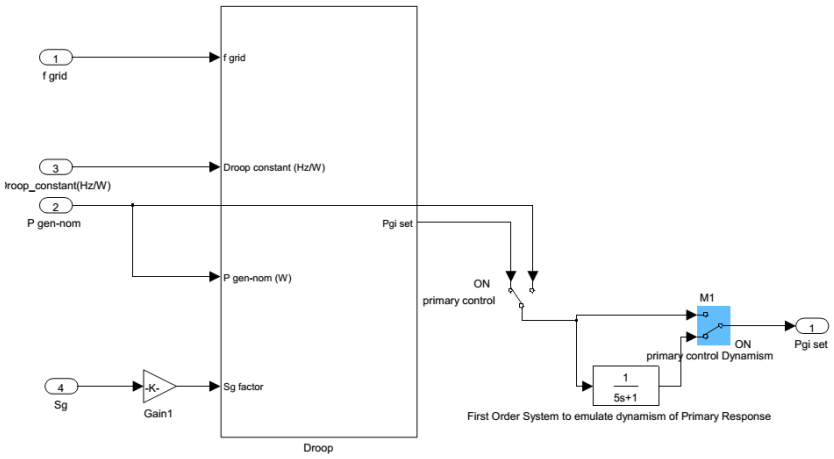

Figure 27 Primary control dynamism

To simulate deployment time delay of primary reserve was emulate using first order system as per guidelines from ENTSO-E. Figure 28 shows effect or simulated deployment time delay of primary reserve.

'A minimum/maximum synchronous area time constant could be set as if it behaved dynamically as a first order filter after the occurrence of a generation-load imbalance.' [12]

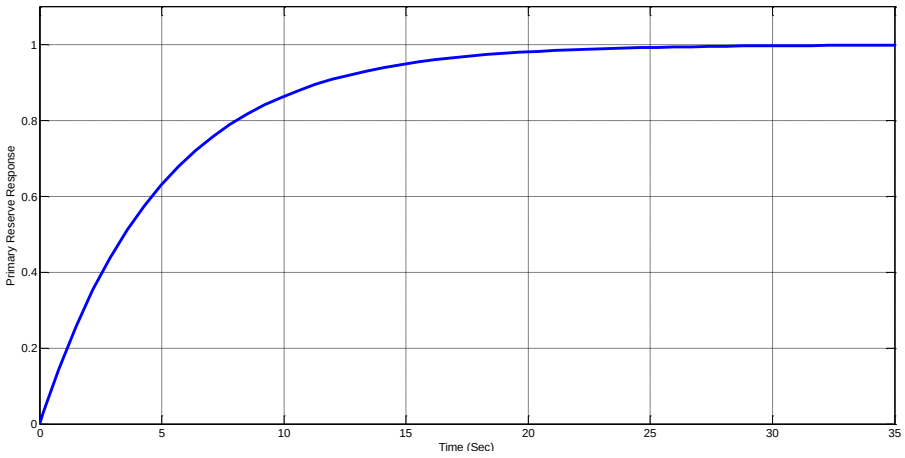

Figure 28 Simulated primary control dynamism

3.2.4. Modelling of self-regulating load

Self-Regulating effect of the load can be defined as percentage load change for every one hertz frequency variation. The typical value of self-regulating load - SRL lies between 1 – 2%/Hz (ENTSO-E, Operation hand book, Appendix-1). Self-regulating Load modelled using following formula

$$\Delta P_{srl} = SRLE * P_{L,0} * \Delta f \tag{3.14}$$

ΔP_{srl} is change in load due to presence of self-regulating load. $SRLE$ is percentage of self-regulating load effect, ΔP_{srl} is load at nominal frequency and Δf is change in frequency.

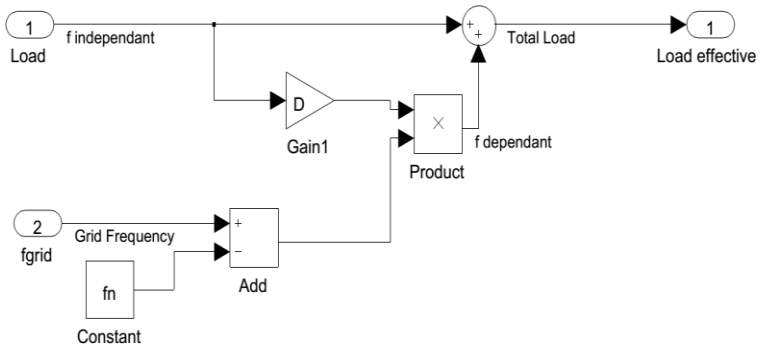

Figure 29 Simulink model of self-regulating load

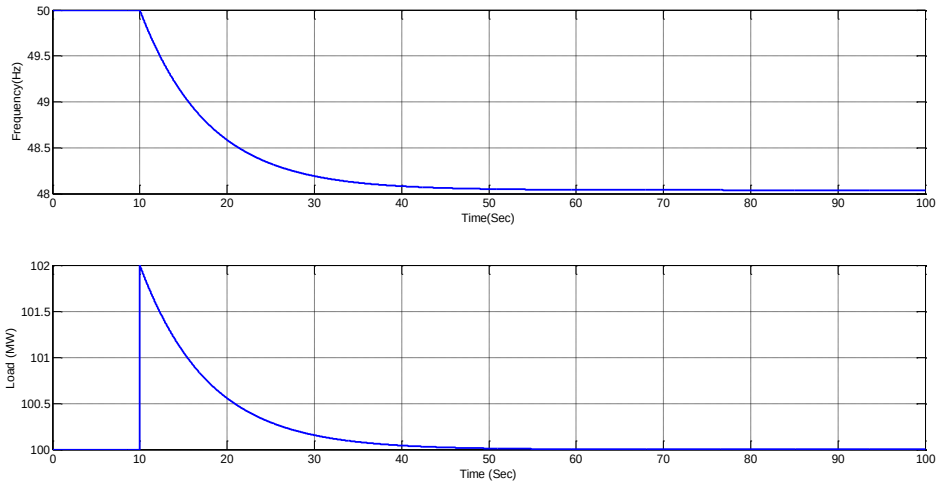

Figure 30 Effects of self-regulating Load

Figure 30 is the result of simulation without any primary control. System has SRL as 1%/Hz. For every one hertz frequency deviation, one percent of nominal power reduction will take place. There was load step of 2MW at 10sec for a system of 100MW (nominal). Assumed no primary control in the system. Due to effect of SRL load was being reduced with respect to reduction in frequency. Finally load reduces 100MW with price of frequency reduction by 2Hz.

3.2.5. Integrated Simulink model

Figure 31 is the global view of model that includes effect of inertia, SRL, λ and primary reserve deployment time.

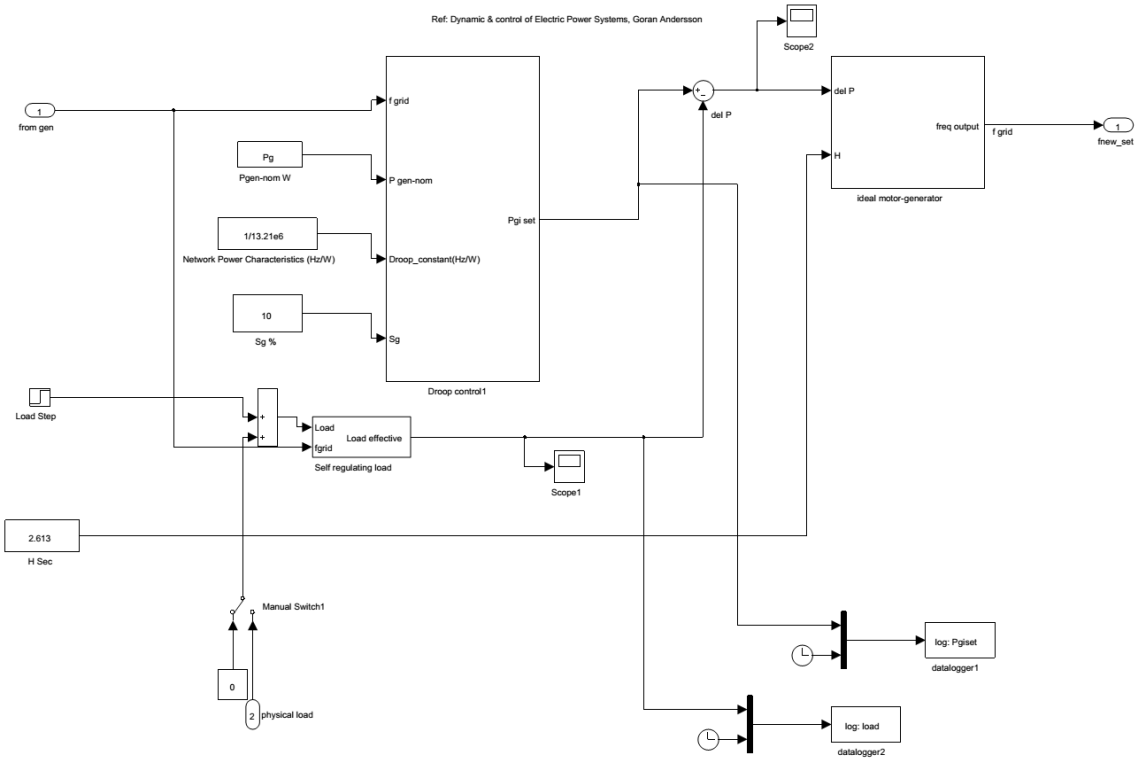

Figure 31 Global diagram of model

In this model, as in figure 31 frequency is fed back to Droop control block and self-regulating load block. Since primary control and self-regulative load performance are depend on actual grid frequency. In PHIL experiment new frequency applied to motor drive and frequency measurement from generator fed back to droop control and SRL blocks.

3.2.6. Input of model

Command window

Ts- Model Sample Time (s)

Pg - Nominal System Power (W)

Fn – nominal frequency (Hz)

PgPC- primary reserve of generator (%)

SRLE – Self regulative Load Effect (%/Hz)

Simulink

λ - Network Power Frequency Characteristics (Hz/W)

Sg – Generator Droop Constant

These are inputs which can be changed for every new grid segment.

3.2.7. Evaluation of integrated simulation result

In this simulation a system with nominal power of 100MW at 50 Hz, load step of 2 MW applied at 70th second, primary reserve of 1%[1], self-regulating load effect as 1%/Hz and network power characteristics as ½ (Hz/MW) .

Load Imbalance = 2MW

Sum of frequency control effect = PC + SRL = 2 + 1 (MW/HZ)

Expected frequency decrease = 50 – (2/3) = 49.33 Hz

[1] In Netherlands by law generation units greater than 60MW should reserve 1% as primary reserve and units smaller than 60MW should have 3% primary reserve. At the same time, primary reserve is not obligatory in Germany. In Germany primary reserve is allotted based on tender [28],[34].

Figure 32 proves the efficiency of model since simulation-result of quasi steady state frequency deviation (49.34Hz) is same as theoretical steady state frequency (~49.33Hz) deviation. However in real time primary control has dynamic behaviour. Figure 32 blue curve shows response grid segment without primary control and green curve represents primary frequency response of grid segment with primary control deployment time model.

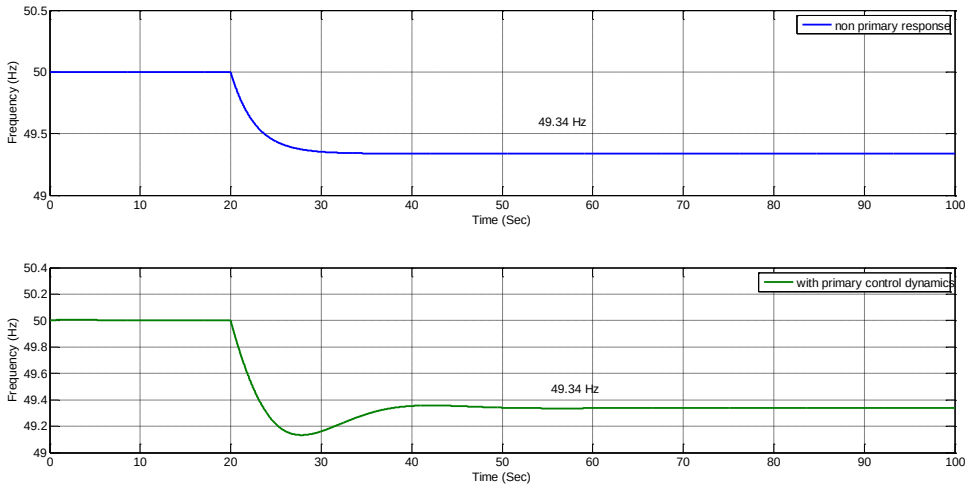

Figure 32 Result of primary control dynamic response

4. Experimental Setup

In this chapter, the experimental setup for PHIL&HIL, calibration methods and result of experiments are discussed. Hardware and simulation can be connected in two different ways in a loop. In first approach, hardware and simulation connected at signal level in the loop. This approach is called as Hardware in the Loop - HIL. In second approach, hardware and simulation connected at power level in the loop. This approach is called as Power HIL.

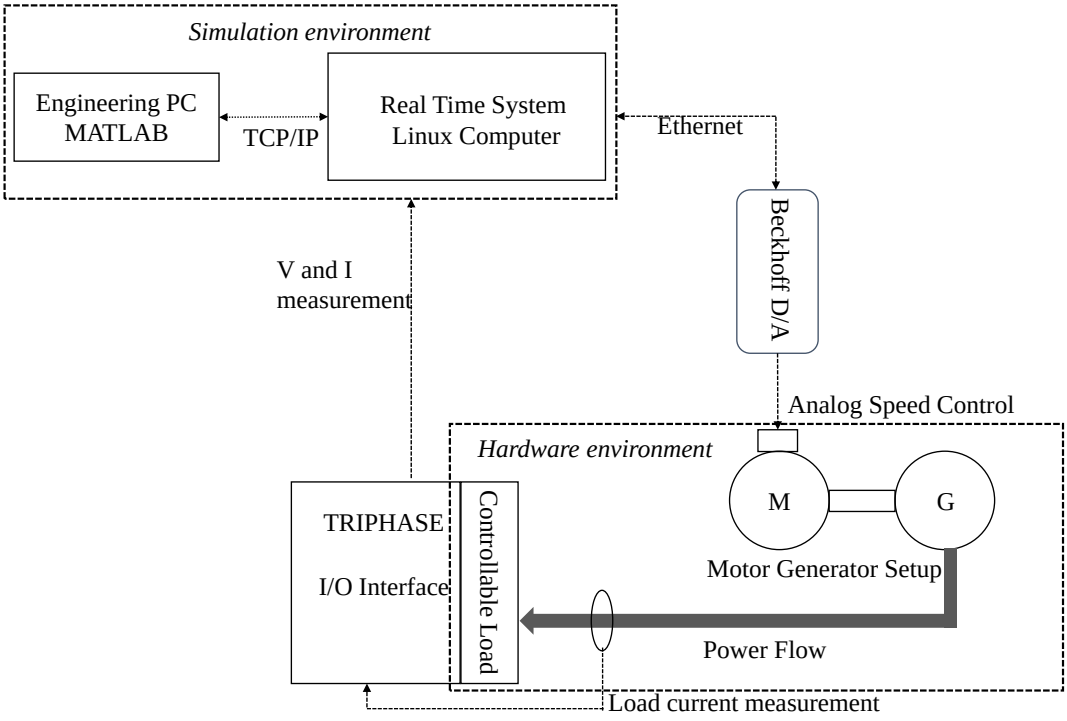

Figure 33 Architecture of PHIL experimental setup

Figure 33 shows the architecture/experimental setup developed for basic PHIL experiment. PHIL experiment is developed based on proper interface between different types of electrical and computing equipment. Computing and measurement equipment were supplied by Triphase ® Company. Though the power converters in Triphase® cabinet were not used in any case of the experiment, the control and communication technologies of Triphase® cabinet were studied to develop initial PHIL experiment. More details about Triphase® were provided in previous section 3.2.

4.1. Introduction

In this section the architecture of PHIL experimental setup is discussed followed by calibration section and result discussion.

Analysing effects of Distribution Energy Resources on existing grid system is attracting more attention now. Researchers wants to test their solutions in real field. However, construction of big power systems are highly cost intensive and time consuming. This problem can be solved by simulating power system in real-time simulator and creating a power interface that emulates the result of areal time simulation. In this experiment generator – motor setup is used as power interface between RTS and resistor load banks.

4.2. Time delays

PHIL experiment is a new concept and is influenced by delays in communication between Digital Real Time Simulator and hardware under test. These problems can be solved by installing fibre optical communication or delay compensation in model. Since my thesis is a basic PHIL experiment and due to the unavailability of digital RTS, these delays were considered as negligible. However, delays involved in experiments were studied for future reference. Key findings of delays are: delay in frequency measurement is 100 ms, in RTS time frame is 0.25 ms and delay in signal communication between Beckhoff module and motor drive is 50 msec. These delays are important findings of this experiment from a stability point of view. These values need to be managed for more advanced PHIL experiment.

4.3. PHIL experiment

Figure 33 shows different types of environment used in PHIL experiment. PHIL architecture is based on two environment, which are

- Simulation environment
- Hardware Environment

Interfacing of these two environment was achieved by motor generator setup.

4.3.1. Simulation environment

Figure 34 explains the purpose of simulation environment in PHIL experiment. It measures generator

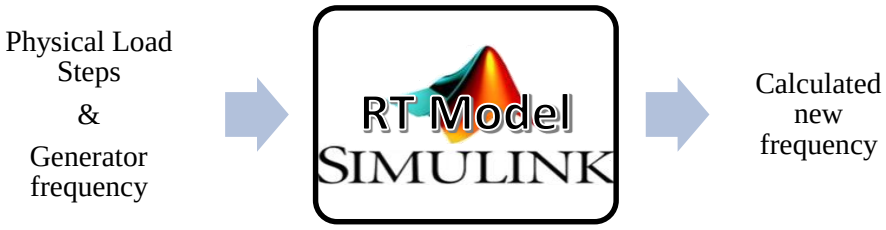

Figure 34 PHIL simulation environment

frequency and load, processes it in real time and calculates the new frequency of generator in real time. One of the main objective of PHIL experiment is interfacing simulation environment with hardware environment in power scale. In PHIL experiment, power flow in hardware affects the simulation results and vice versa. In this experiment, simulation environment is created by RTS and engineering PC. More details about simulation models were explained in section 4.2.2. In the simulation environment, inertia, self-regulating load, droop control and primary reserve deployment time were modelled. Simulation environment has two computers, out of which RTS plays major role in real time and the Engineering PC acts as an interface between researcher and RTS. Inputs are supplied to Engineering PC and communication established with RTS by Engineering PC with help of MATLAB external mode. At the same time, engineering PC gathers measurement data from RTS and displays it. The real time communication link between RTS and Engineering PC was established by MATLAB external mode and TCP/IP protocols. Speed of TCP communication is in the range of 1-10 Hz hence the data displayed on Engineering PC is not time critical. The Time critical data were logged in RTS and it can be downloaded. It is evident that during experiment, all real time tasks were handled by RTS.

4.3.2. Hardware environment

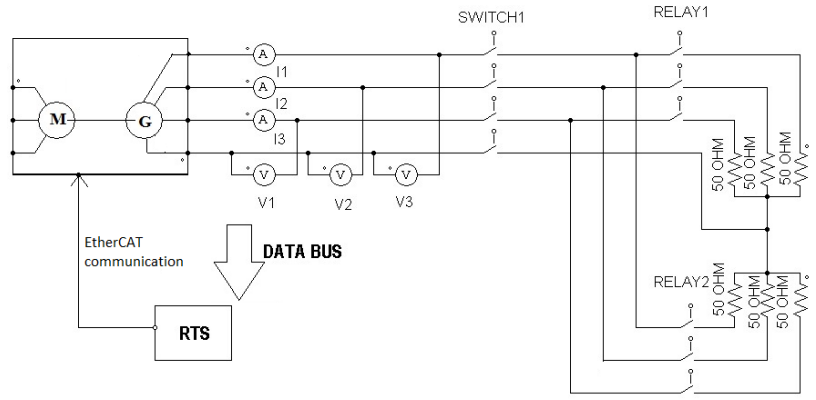

Figure 35 PHIL experimental setup

Figure 35 shows the experimental setup and power connection among hardware used in PHIL experiment. Experimental setup has a motor generator setup, measurement devices from Triphase® cabinet, controllable loads and RTS. There were Ethernet communication established among different devices for real time communication. Controllable load is one of the basic requirement to implement an initial PHIL experiment. More details about design of controllable load is described in section 4.3.2.1.

The motor generator setup was connected to 3kW symmetrical resistive load bank by contactors. Current and voltage sensors measures generator output current and voltage and feedback it to RTS. Based on feedback signals RTS determines reference speed to motor drive. The resistive loads is considered as laboratory network. In future this network will be expanded for more complex PHIL experiments.

52.5 kVA generator connected with 22 kW motor. Motor has CFW -11 motor drive. The motor drive was set in remote mode and is controlled by an external analog signal. The programmed settings were 0-10V for speed change of 40-75Hz. By controlling analog voltage, the speed reference to motor can be changed thus motor operational speed can be controlled remotely. The analog signal to motor drive needs to be controlled in real time and this challenge was solved by controlling motor drive with Beckhoff EL4004. More details about EL 4004 available in Appendix A.7.

The speed reference for motor drive is set by RTS computer. RTS gathers data from Voltage and current sensors in real time. Voltage and current sensors are interfaced with RTS via FPGA boards in TRIPHASE inverters. By using PLL, model measures current frequency, calculate new frequency in 0.25 ms and control Beckhoff output voltage.

Figure 36 is the overall experimental setup view. Power and communication flow diagram of PHIL experiment available in appendix A.8.

Figure 36 Laboratory setup

In PHIL experiment controllable load used to evaluate effectiveness of experiment. Section 4.3.2.1 is dedicated for design and control of controllable loads.

4.3.2.1. Controllable load design

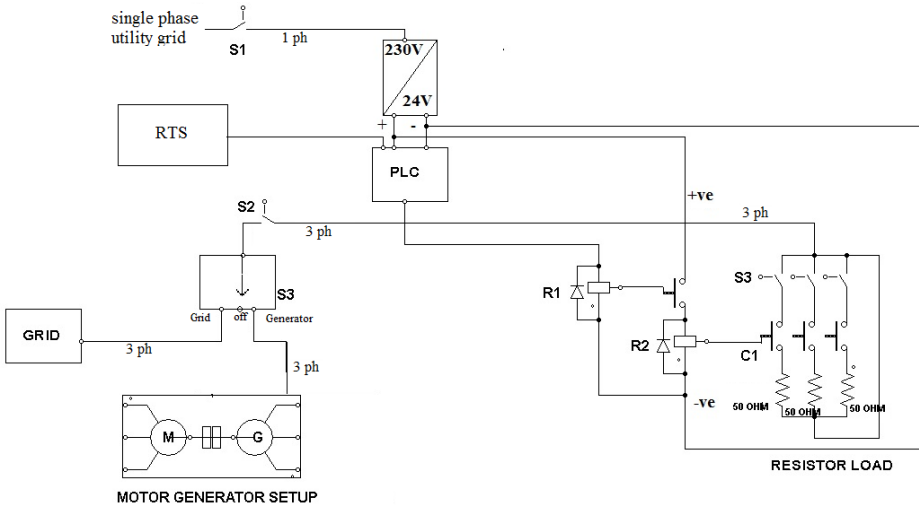

Figure 37 Design of controllable load

4.3.2.1.1 Introduction

In PHIL experiment, the availability of controllable loads are inevitable; since to test the model, the simulation environment should be affected by changes in hardware. Controllable loads creates power flow changes in hardware. The design of controllable load was developed by using three 50Ω resistive loads, relay, contactors, PLC and RTS. It is important to control loads in real time, though in this experiment controlling of load in real time is not necessary, in future automatic demand side load management would be developed in PHIL environment. This real time load control decision was made to generate experience and interface technology for future developments. In this experiment Controllable load was not controlled by any intelligent algorithm.

4.3.2.1.2 Design

Figure 37 is the design developed for real time controllable load. Resistive load of 3 kW was chosen to act as controllable load. It was assumed that voltage is always 230 V. Hence, frequency change is only affected by change in active power. Resistive loads were chosen to consume active power. As shown in figure 37, resistors with value of 50Ω were connected in star connection. Switch S3 acts as the power source selection switch. By adjusting S3 the experiment can either be powered by utility grid or by motor generator setup. Since it is important to control power source frequency, S3 is always connected with generator. Grid power was used only for calibration procedures. Resistor bank is connected to S3 via R2C1 contactor. Hence by controlling R2C1 the active power consumption in the experiment can be

controlled. It is necessary to control R2C1 in real time. In other words, R2C1 needs to be controlled by RTS. Hence, EL2008 Beckhoff module is used to establish connection with RTS. Beckhoff module connected with RTS in Ethernet communication link. The update time of Ethernet communication is 50 ms. Beckhoff module was interfaced with RTS by BusXMLEditor provided by Triphase®. More details regarding fieldbus can be found in XMLfile at appendix A.4. R2C1 contactor cannot be driven directly by Beckhoff module. Beckhoff module cannot provide enough current to drive R2C1. Hence a driving relay R1 is added to circuit. R1 is controlled by Beckhoff module. Once R1 is activated by Beckhoff module, it will energise R1C1 thus it closes the power flow from source to load.

4.3.2.1.3 Delays in controllable load design

Operating time of LC1DT25 (R2C1) is 12-22 ms for closing and 4-19 ms [36] for opening the contactor. For primary relay 114A-424VDC1L (R1) operating time is approx.10 ms [26]. For controlling loads in introduces delay of approximately 20-30 ms. At current experiment setup this time delay does not cause instability uses but in future more complex design should include compensating circuit for this delay.

4.3.3. Calibration

It is important to calibrate all measurement devices before conducting any experiments and analysing any result.

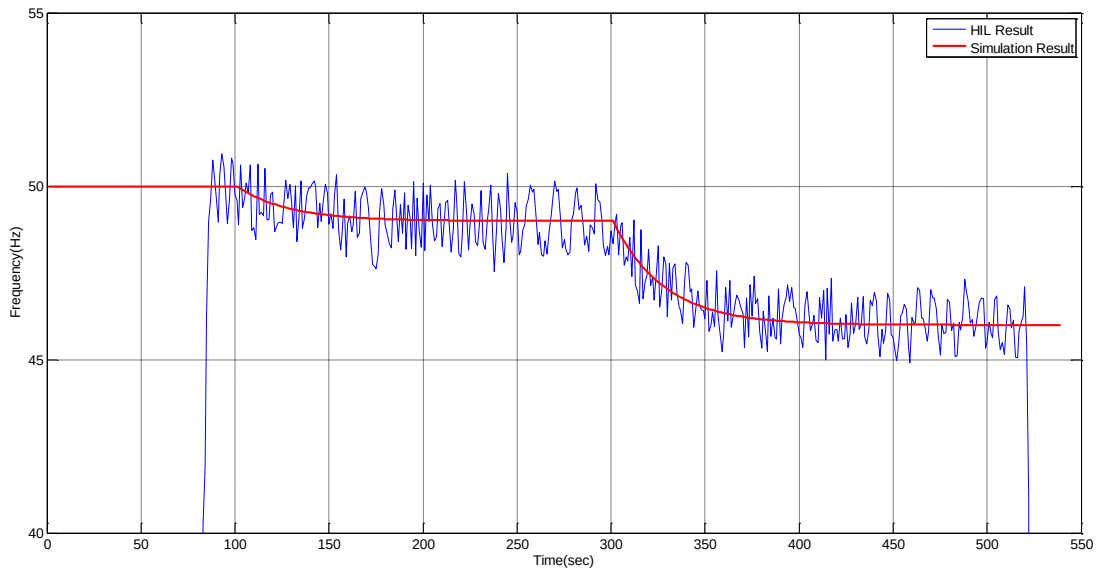

Figure 38 Non-calibrated frequency measurement

4.3.3.1. Frequency measurement calibration

Figure 38 is the result of open loop frequency measurement test, in which generator forced to operate at 50Hz, 49Hz and 46Hz; the Red line in figure 38 denotes result of complete forward simulation and the Blue line denotes measured generator frequency. It is important to note that in this experiment measured frequency from generator was not fed back to simulation in real time. Thus this experiment there is neither HIL nor PHIL. The Purpose of this experiment is to calibrate frequency measurement and data logging. It is clear that Generator output frequency follows simulated values however frequency measurement was highly distorted, it has accuracy of ±1.5Hz from actual measurement. This is the status of result of initial experimental setup. Measures were developed to calibrate frequency measurement, which are frequency measurement using PLL was averaged over five cycle fundamental frequency (0.1 s) and slow data logging in RTS.

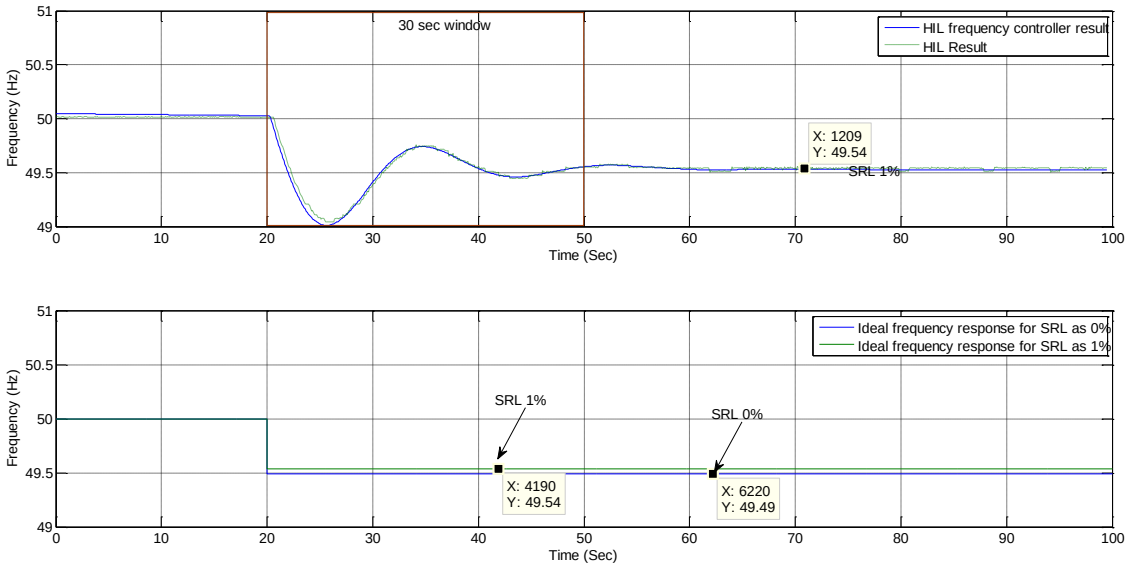

Figure 39 Emulation of 2006 grid disturbance

Figure 39 explains calibrated frequency measurement, in which HIL frequency measurement closely follows simulation result. More details regarding figure 39 was discussed in section 4.4.3.

Figure 40 is the result of open loop test, in which generator forced to run in steps of 48.0, 48.5, 49.0,

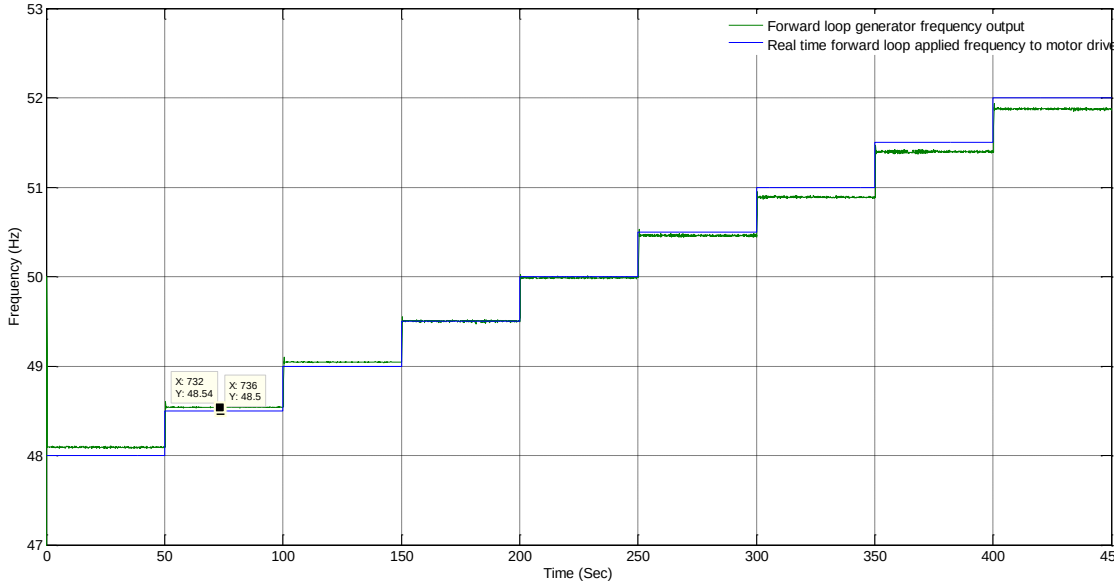

Figure 40 Applied and measured frequency

49.5, 50.0, 50.5, 51.0, 51.5 and 52.0 with time step of 50seconds. In ideal motor drive situation, generator will operate at any given frequency. But in real time, generator output frequency accuracy varies. This effect can be observed from figure 40, where difference between applied (blue) and measured frequency (green) varies when frequency deviated from 50 Hz. It can be either due to Phase Locked Loop frequency measurement or motor-generator intrinsic error or mechanical constrain or controller of motor drive. The performance of PLL was tested by comparing PLL measurement with third party smart power meter EM 133[1]. It was found that frequency measurement from both PLL and EM 133 is similar with error of ±20 mHz - ±100 mHz. It can be concluded that PLL performance is satisfactory. It leads to the decision that difference in frequency measurement is caused by offset in controller of motor drive or mechanical constrain. This frequency error needs to be calibrated. Since this thesis is based on PHIL experiment development, it was decided to use PHIL frequency feedback to compensate for this frequency error. In other words, real time frequency measurement from generator output terminal is fed back to Simulink

[1] This 50 Hz operation is verified by external power meter SATEC - EM 133®.

model. Since Simulink model has controller for primary control of grid, the offset error introduced by motor drive or mechanical constrain is compensated and required frequency of operation is obtained. Improved frequency tracking can be observed from 48. In which measured frequency closely follows simulated frequency.

4.3.3.2. Power measurement calibration

4.3.3.2.1 Problem due to un-calibrated load measurement

Due to noise in voltage and current measurement since they rated for 1.3kV and 0.25-50A respectively. The noise cause poor load power measurement. Thus there was difference in supply and demand that leads to frequency 50±0.2 Hz.

In figure 41, load measurement shows noisy power measurement, which will affect the accuracy of PHIL

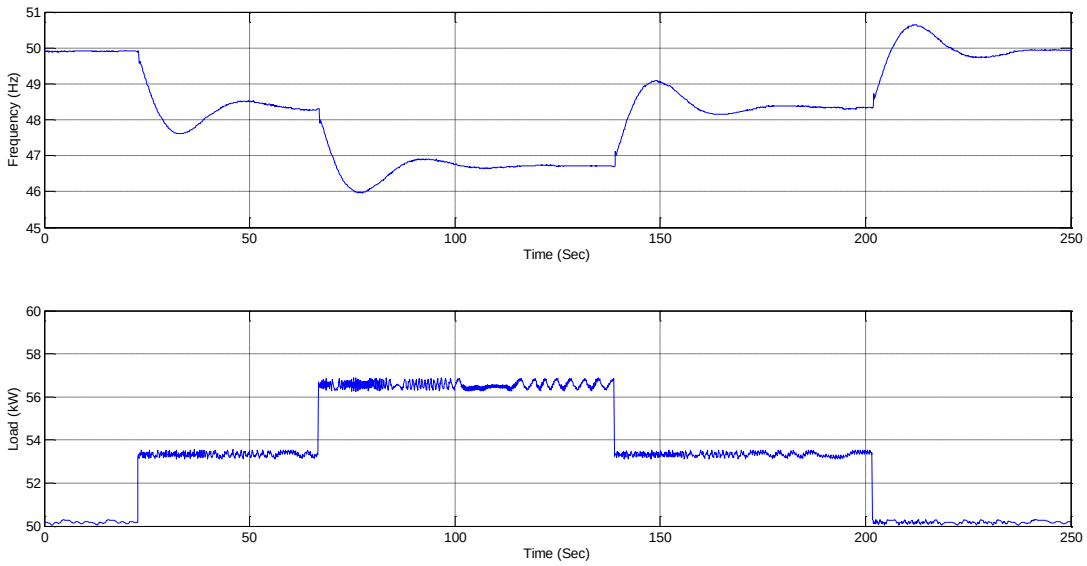

Figure 41 Result of non-calibrated PHIL experiment

experiment. Measurement sensors needed to be calibrated for efficient PHIL experiment. In this thesis PHIL experiment uses two 3 phase symmetrical resistive load (wire wound resistors) rated 3.174 kW and simulated offset power of 50kW. In non-calibrated situation power measurement can be observed from right column of figure 42. Non calibrated power measurement were noisy in the range of 400W (12.6% error). Ideal power was calculated as 3.174kW, for constant phase to neutral voltage as 230V and 50Ω load per phase. Figure 42 shows deviation of measured value from ideal load for both calibrated and non-calibrated load power measurement. Measures including RMS calculation and offset were deployed to reduce inaccuracy of power measurement. Thus accurate power measurement in experiment was improved, which can be observed from left column of figure 42. Calibrated power measurement had error of 0.6% compare with ideal load of 3.174 kW.

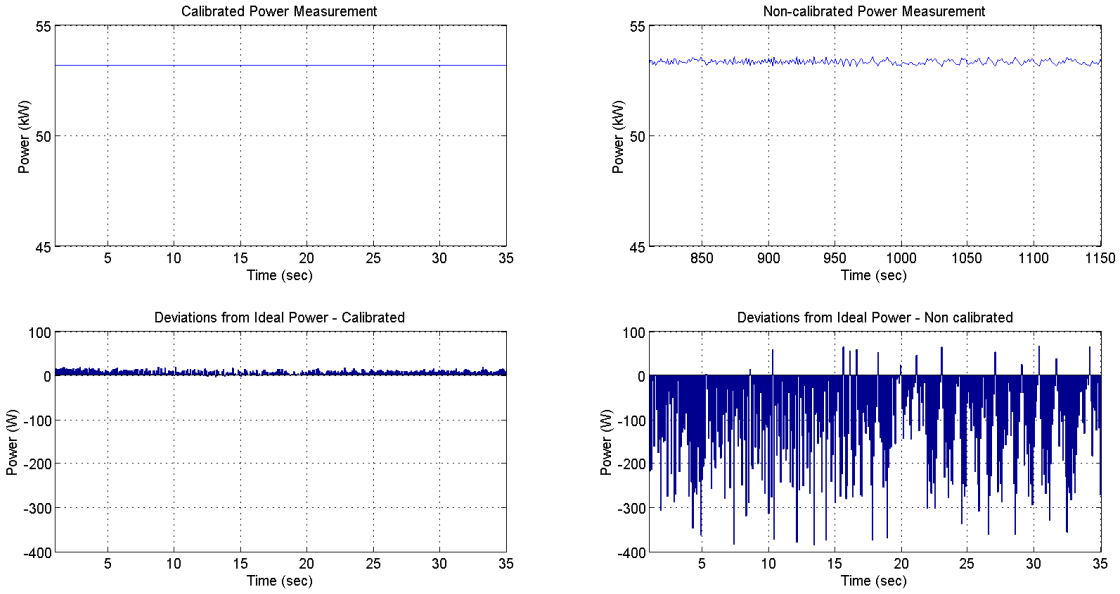

Figure 42 Power measurement calibration

4.3.4. PHIL experiment

In this section, PHIL experiment conducted for hardware load of 6.3 kW and its impacts on 50 kW nominal grid segment with λ of $^{1}/_{2}\,\frac{Hz}{kW}$

4.3.4.1. Introduction

In complete PHIL experiment 'transfer' of power maintained between simulated network and hardware. Power flow interface plays a major role which ensure power flow in real time. In this experiment power consumption of resistive load is measured and fed back to simulation environment in real time. The real time power measurement is facilitated by measurement sensors in Triphase® cabinet. Change in real time hardware power consumption has effect on simulation in real time. This section tries to validate this argument.

Model was running in real time at RTS meanwhile physical resistive loads were switched on/off to analyse the response of simulation environment and output frequency of generator. In normal operation

condition, to maintain nominal frequency of operation at terminal of generator, supply demand gap[1] need to be maintained to be zero. To maintain supply demand gap as zero, offset load of generator nominal power of 50 kW was simulated. Whenever a physical load change occurs the current sensors and voltage sensors measures changes and communicate to RTS via FPGA. The RTS will analyse changes in load current and based on model, calculates new frequency. It is important to note that in this emulation new frequency is calculated based on real time load change.

4.3.4.2. Test case evaluation

In this test case, network power frequency characteristics λ assumed as $\frac{1}{2}$ $(\frac{Hz}{kW})$, 50kW considered as nominal power of a grid segment for 50Hz operation and inertia assumed as 4 s. First order system with time constant of 5 used as primary reserve deployment time model. In real time, in a power system if a supply does not match with demand there will be frequency disturbance. In this case for time 0-50 s supply is assumed to be equal to demand of 50kW of simulated load. As in figure 43, around 60 s

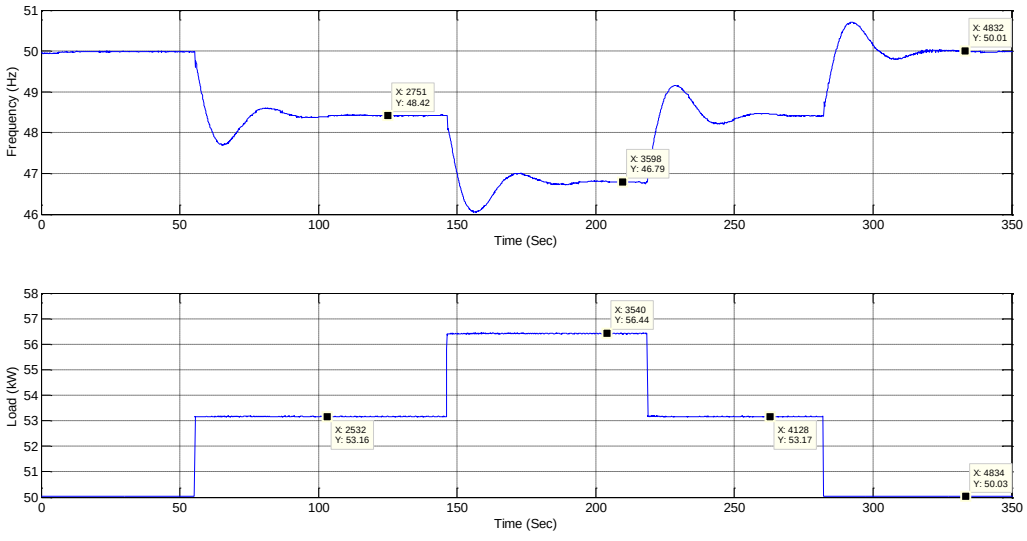

Figure 43 Result of basic PHIL experiment

[1] Losses in transmission assumed as zero.

physical resistive load of 3.174kW turned on[1]. In ideal condition, this 3.174 kW causes quasi steady state frequency as 48.413Hz also in experiment generator output frequency measured as 48.42Hz.

Around 140 additional load of 3.241kW turned ON. In ideal case, quasi steady state frequency is 46.7925 Hz and PHIL resultant frequency also reached 46.79Hz. Thus quasi steady state results of ideal case and PHIL experiment result were similar. After 200 s two loads were turned off one by one and frequency return to 50.01Hz. As shown in figure 33, in this experiment, there were two hardware were used which are generator and resistive loads. Those two hardware, RTS and other I/O device created a closed loop. In this experiment, the motor-generator set acted as power interface and power flow in resistor causes changes in simulation environment. Since simulation environment represented by generator, frequency of generator varied for varying power flow in laboratory network (resistive load). Figure 43 clearly explains change in generator output frequency for change in load power consumption and hence proves the basic PHIL experiment accomplished an efficient result.

[1] Since Automatic Voltage Regulator is installed in generator, generator output voltage remains constant even though load increases.

4.3.4.3. Accuracy of PHIL experiment

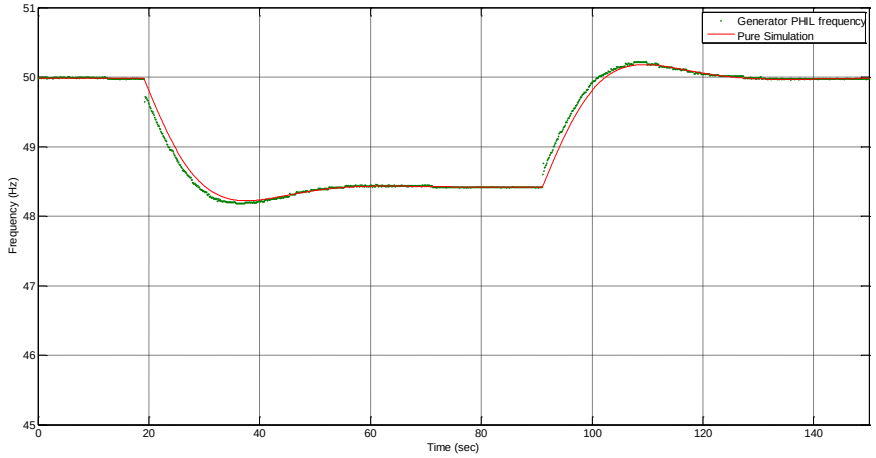

Figure 44 Comparison of PHIL result and simulation result

In this section overall accuracy of PHIL experiment is discussed. In previous section it explained about steady state frequency values. Figure 44 explains the accuracy of PHIL experiment including dynamic frequency variation of PHIL result and simulation result. In ideal case, both curves should be identical. However due to sudden torque change in motor drive the simulation curve and actual PHIL experiment result were slightly deviated.

Figure 45 explains accuracy of overall experiment, 0 Hz denotes zero error between simulated frequency and actual PHIL experiment result. However due to PLL and sudden torque changes the deviations exists in experiment. It can be solved by programming motor drive in tighter constant torque mode and creating more efficient PLL for frequency measurement.

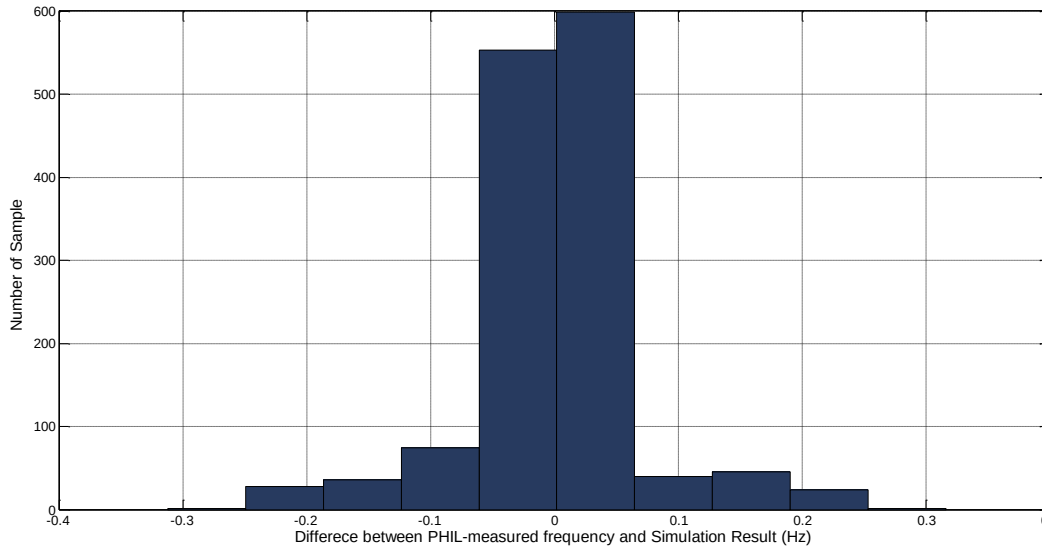

Figure 45 PHIL experiment accuracy

4.4. HIL experimental setup and result discussion

HIL experiment is following same concept as Power HIL experiment. In this thesis work basic difference between power HIL experiment and HIL experiment is, in PHIL experiment load steps are real but in HIL experiments loads steps were simulated. Figure 46 shows experimental setup used for HIL experiments.

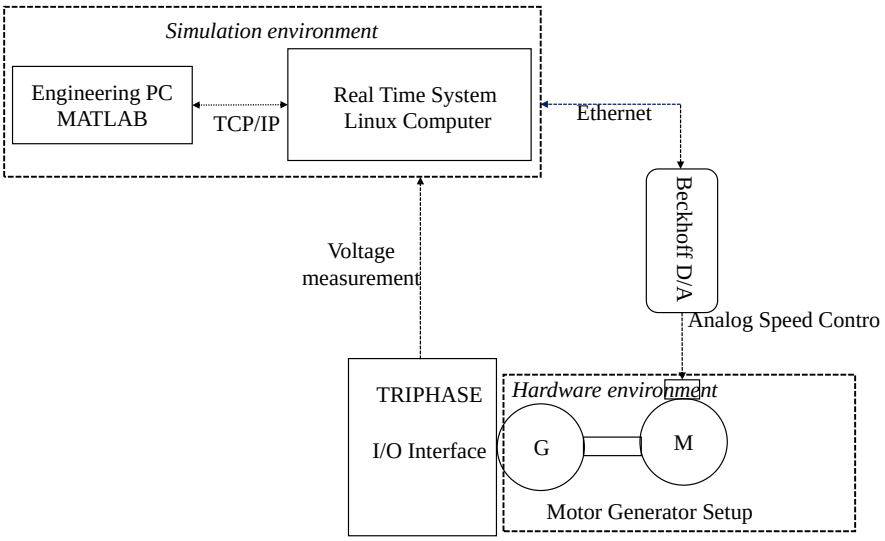

Figure 46 Block diagram of HIL experimental setup

In this section emulation of frequency response of power systems using the motor-generator set as hardware in the loop is discussed. Since hardware connected with simulation environment is in signal level (Beckhoff module), this emulation can be considered as a basic HIL experiment.

4.4.1. Simulation environment

Figure 47 explains simulation environment of HIL experiment. It can be noted that HIL experiment uses simulated load steps.

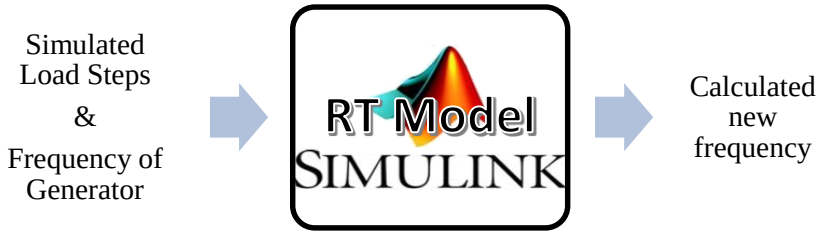

Figure 47 HIL simulation environment

4.4.2. Hardware environment

As shown in figure 48, It is explicit frequency of utility cannot be controlled by researcher so throughout the experiment motor-generator setup was used to emulate variable frequency. Voltage sensors are

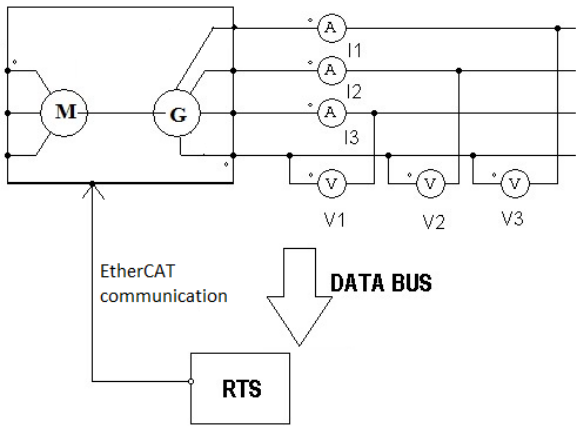

Figure 48 HIL hardware environment

interfaced with RTS via FPGA and Ethernet communication. RTS measures frequency of generator using PLL to analyse voltage signal and calculates new frequency using Simulink model explained in section 3.2. RTS controls generator frequency by Beckhoff module. Communication between Beckhoff module and RTS is established with EtherCAT communication.

4.4.3. Procedure

Model was developed in engineering PC and exported to Real Time PC, in this step the simulation will be converted into C code and uploaded to RTS for real-time simulation.

In Engineering PC, load steps were simulated that affects model in RTS and calculates new frequency and RTS controls motor drive thus frequency of generator. In this case generator output frequency is measured by analysing external voltage measurement across output terminal of generator and the frequency values will be logged for later analysis.

The results of two HIL experiment cases were discussed in sections 4.4.3 and 4.4.4.

Current HIL experiment generated knowledge for possibilities of interfacing digital RTS and hardware. In future, if digital RTS is used, the more complex design such as real time power and load generation data can be communicated to digital RTS.

4.4.4. Case1: Evaluation of model by grid disturbance on 2006

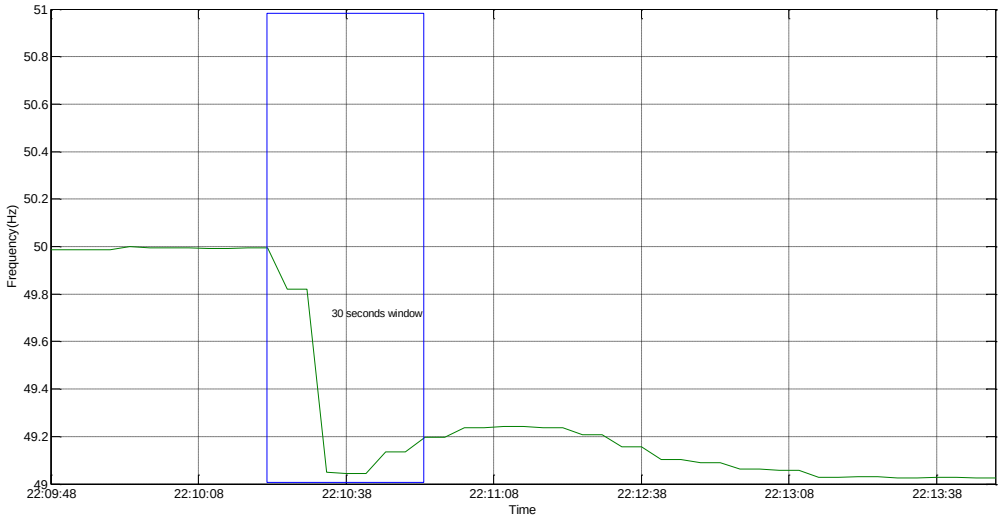

Figure 49 Case 2006 Western part of EU grid disturbance

The efficiency of Simulink model developed in this thesis evaluated by recreating frequency disturbance occurred on 04 Nov 2006. In figure 49, the actual grid disturbance occurred on 2006 is showed. During the event on 04Nov 2006, UCTE EU grid split into three section as in figure 16. In this section, frequency behaviour of western part of EU continental grid was tried to recreate for first 30s since event occurred. The frequency data during disturbance was provided by TenneT.

4.4.4.1. Parameters for primary frequency response of grid

It is not possible to design power system in GW range in laboratory scale. Hence, parameters that affects grid primary frequency response behaviour need to be found and educated assumption have to be taken to emulate frequency behaviour of grid segment for given event. Following parameters are major parameters that determines primary frequency control behaviour of behaviour of grid during disturbance.

- Supply Demand Gap
- Total generation capacity
- Network power frequency characteristic (λ)
- Grid inertia constant (H)
- Deployment of primary control reserve
- Percentage of Self Regulating Load

Generation profile and demand profile of western region during the event were not available hence it was decided to use a supply demand gap data, which was found as 9000MW[1] [18]. The 9000MW supply-demand gap caused only by loss of transmission facilities with separated eastern and southern grids. However, the frequency drop increased by additional tripping of generation and tripping of 60% of connected wind energy and 30% of connected CHP, which further widen supply demand gap; which constituted generation loss of 10900MW.

4.4.4.2. Model constraint

The set points of frequency relay at wind farms substation or power electronics set points in wind farm caused disconnection of wind farms during grid disturbance. The model developed in this thesis does not include model of inverters for wind power generation or CHP. It is difficult to collect accurate supply demands gap during the event, because during the event different TSO implemented different protective mechanisms such as load curtailment and shutting down of pumped hydro. In absence of this data, precise recreation of the given event is not possible.

It can be perceived that the initial 9000MW supply demand gap was not constant throughout grid disturbance duration. The supply demand gap was dynamically changing, based on loss of generation and control actions by TSO[2]. Since the dynamic supply demand gap was not available, it is necessary to develop model that includes different generation and transmission lines to exactly mimic frequency disturbance during 2006. The detailed model[3] is not objective of this thesis and available computer power also restricts more complex real time model.

[1] It was important to notice that all primary reserves are calculated for loss of 3000MW of generation.

[2] Control actions: control of pumped storage or activation of secondary/tertiary control reserve

[3] Detailed model needs to be developed in real time computer; the current computing power at Renqi laboratory is one CPU. Detailed model may require high computing power, which can be supplied by RTDS or Opal- RT. The RTDS and Opal-RT have number of parallel CPU to handle high computing load in real time.

4.4.4.3. Expected behaviour

In conclusion, since dynamic supply demand gap data for 2006 disturbance was not available it was assumed supply demand gap as a constant 9000MW. Hence, model can emulate behaviour/profile of frequency disturbance but the actual quasi steady state frequency values of real event and simulated event cannot be same.

4.4.4.4. Parameter scaling

Network power frequency characteristics of UCTE grid on 2006 was 26434 MW/Hz [2]. The total generation before disturbance was 274100MW. After disturbance UCTE grid separated thus three grid segments were created with different frequencies, in which western grid segment is the focus of this experiment. The western grid segment had generation of 182700MW before the event. Primary control reserve distribution depends on annual energy generation of given grid segment. However, in normal operation western grid segment does not exist so data regarding energy generation of western grid segment was not available. Hence it was assumed primary reserve was distributed based on instantaneous power generation before the event. It leads to primary reserve – network power frequency characteristics (λ) of western grid segment as 17619MW/Hz. Inertia of grid assumed as 7s. Also it was assumed that Total generation capacity of western grid was found as 182700 MW [41] Self-regulating load effect assumed as 1%/Hz since in ENTSO-E simulation, they used 1%/Hz [14]. Table 4 explains the assumption made for recreating the event.

Table 4 Laboratory assumption for emulating 2006 grid disturbance

Parameters	**Laboratory assumptions**
Supply Demand Gap	9000MW
Total generation capacity	182700 MW
Network power frequency characteristic (λ)	17619MW/Hz.
Grid inertia constant (H)	7 s
Self-Regulating Load	1%/Hz
Response time of primary control reserve	First order system with time constant of 5 s

4.4.4.5. HIL result and discussion for 2006 grid disturbance

By analysing figure 49 and figure 50, it was clear that in both figures frequency drops as soon as grid disturbance occurred. In real event after ~12 s frequency started to recover. The slope of frequency drop was controlled by inertia and SRL. But in real event since supply-demand gap exceeds reference incident number of protective mechanism were kicked in and controlled the rate of change of frequency. But in

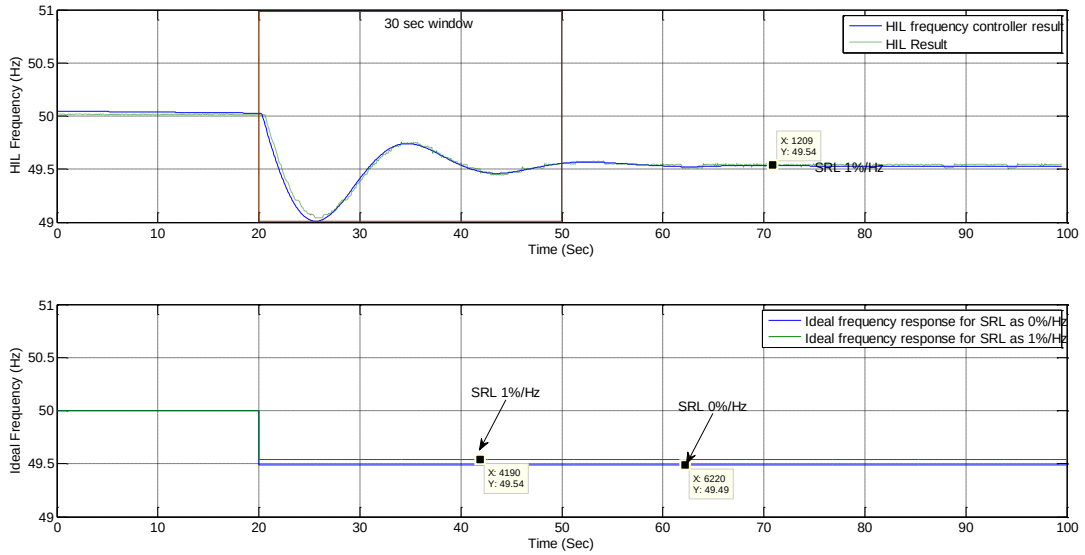

Figure 50 Emulation of 2006 grid disturbance

HIL result slope was controlled by inertia and SRL. In both figures 49 and 50 the frequency response profile drop for an event is similar.

In real time event frequency started to recover after 12 s. But in HIL result frequency started to recover around 8 s. The HIL model is developed for generic grid, generic grid disturbance and model followed ENTSO-E grid codes. ENTSO-E regulated primary reserve should be available within 30s. HIL model used first order filter with time constant of 5 s to emulate the deployment time of primary reserve. But in real event primary reserve takes more than 30 s for complete deployment. This behaviour can be emulated by increasing time constant of first order filter. But this will breach ENTSO-E grid codes. Hence, time constant increased-first order filter was not used in this simulation. After event, frequency stabilises and quasi steady state value achieved. From figure 50, the quasi steady state value of HIL frequency is similar to ideal frequency. It proves system's performance is efficient. Ideal frequency plot in figure 50 clearly explains the impact of SRL in quasi steady state frequency value. Thus recreation of 2006 grid disturbance profile is an efficient result.

4.4.5. Case2: A potential solution: Wind turbine inertia in Aruba

In this section, experiment to emulate the behaviour of grid segment and effect of wind turbine inertia are experimented. Though this section is based on ambitious technical assumption, it can be possible in future. Since in Northern grid Nordic grid code insists the possibilities to explore primary and secondary control in wind energy. In other words, it is necessary for Aruba to explore all possible to increase grid stability solutions to achieve its ambitious goal of 100% energy independency from Oil.

The overall installed capacity of Aruba is 320.4 MW, details are tabled in appendix A.9. The data related to primary control and inertia is not available. Following section will explain educated assumption for network power frequency characteristics (λ) and inertia (H) constant.

Average demand of Aruba is 103 MW and peak demand reach up to 125MW [44]. Since unit commitment details are not available it was decided to make assumption for unit commitment during peak demand. RECIPS based engines in Aruba are 30% efficient compare with turbine generators it was decided to cover ~50% demand with high efficient unit. It is assumed that Wind Turbine are at peak generation of 30MW. The 30MW wind generation is assumed since this is worst inertia situation possible for Aruba for high penetration of renewable energy; by preparing for worst situation, Grid can handle any other situation less severe than this.

Table 5 Assumed unit commitment for units in Aruba

Generator Type	Capacity	H(s)
1 × 35 MW Turbine Generator	35 MW	3.3
2 × 8 MW RECIP Generator	16 MW	3.5
4 × 11.3 MW RECIP Generator	45.2 MW	3.5
Vader Piet wind park	30 MW	0
Cumulative Installed Capacity	126.2 MW	2.613

Table 5 explains the assumed unit committed units in Aruba column titled H[1] is the inertial constant of respective units with respect to their rated power. It can be noted that Vader Piet wind park has zero inertia constant at current situation. The effective inertia constant of grid of Aruba calculated by assuming all generators connected with transformers that has unlimited transfer capability. It found that inertia constant for Aruba for given unit commitment is 2.613 s. The network power frequency characteristics for Aruba is not available hence it is decided to find network power frequency characteristics (λ) of Aruba by extrapolating λ of Netherlands to Aruba's[2] installed capacity.

Installed Capacity of Netherlands on 2013 22429MW [40] and Network Power Frequency Characteristics (λ) of Netherlands for 2013, 1020 $\frac{MW}{HZ}$ by linear extrapolation λ for Aruba found as 13.21 $\frac{MW}{HZ}$.

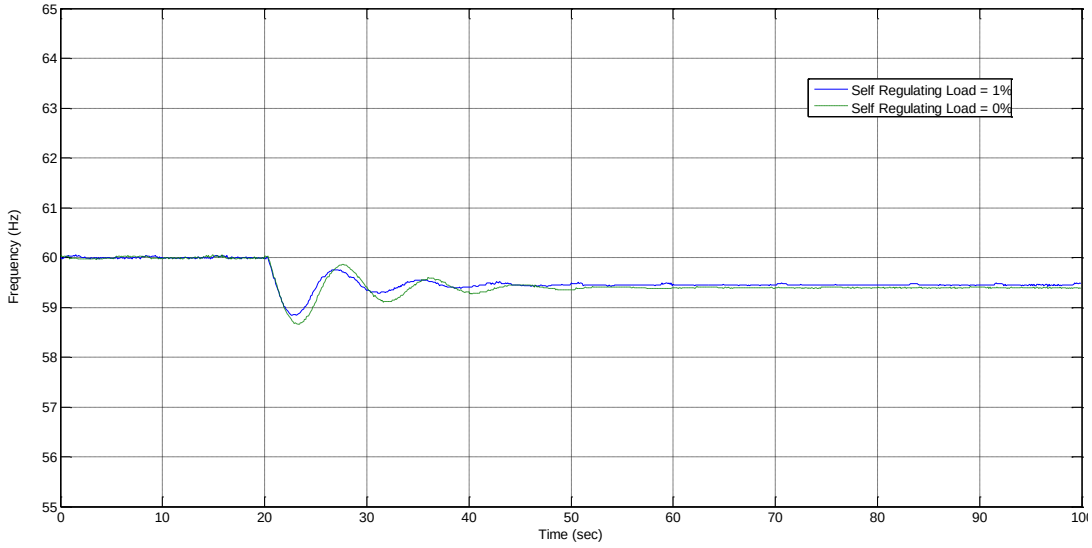

Figure 51 Aruba frequency behaviour for generation loss of 8MW at 20 s for SRLE as 0% and 1%

[1] The H value for respective power plants were used from (Kundur) and (Pieter Tielens). Please refer appendix A.10 for more details

[2] Aruba is a part of Netherlands Kingdom

It was assumed that primary response reserve in Aruba grid system follows first order system response with time constant of 2 s. In modelling section, it was argued that model is capable of emulating effect of self-regulating loads. Figure 51 is the result of HIL experiment for emulating Aruba grid system for loss of an 8MW generator. Two scenarios were emulated. First scenario, had 0%/Hz self-regulating load and in second scenario it was 1%/Hz[1] self-regulating load. Scenario with 0%/Hz of SRL had maximum dynamic frequency deviation[2] of ~1400 mHz whereas scenario with 1%/Hz has maximum dynamic frequency deviation of ~1150 mHz. For scenario with 0%/Hz SRL, quasi steady state frequency[3] for Aruba for loss of 8MW generation is 59.394 Hz (theoretical value); the experiment result was 59.3896 Hz. For scenario with 1%/Hz SRL, quasi steady state frequency for Aruba for loss of 8MW generation is 59.4472 Hz (theoretical value); the experiment result was 59.4589 Hz.

Figure 51 shows, both quasi steady state value and maximum dynamic frequency variation is being reduced for increase in SRL.

Wind turbine inertia

In this section, the effects of using inertia of wind turbines are discussed. It is evident that mass associated in wind turbine and generator has inertia of its own. In this section, only inertia of wind turbine is considered. Current market practices and technology does not use the inertia of wind turbine. In this experiment, it was assumed that wind turbine generator, transformer, transmission line other electrical equipment have infinite ratings to provide sufficient active power to grid. The grid inertia constant of Aruba is increased by ~1.43 s compare with current inertia constant value.

Frequency behaviour of grid of Aruba for current scenarios and scenario with wind turbine inertia were simulated and results are shown in figure 52.

[1] It was noted that Aruba is an island and main stream of economy is driven by tourism. Penetration of SRL for Aruba would be less.

[2] When grid undergoes frequency disturbance, before frequency reaches quasi steady state value it may swing. Maximum value of the swing called as maximum dynamic frequency deviation. This swing depends on stability of system.

[3] When supply demand gap occurs, grid frequency gets disturbed. According to ENTSO-E regulation grid frequency may drop to ±200 mHz for maximum of 30 s. This frequency called quasi steady state frequency.

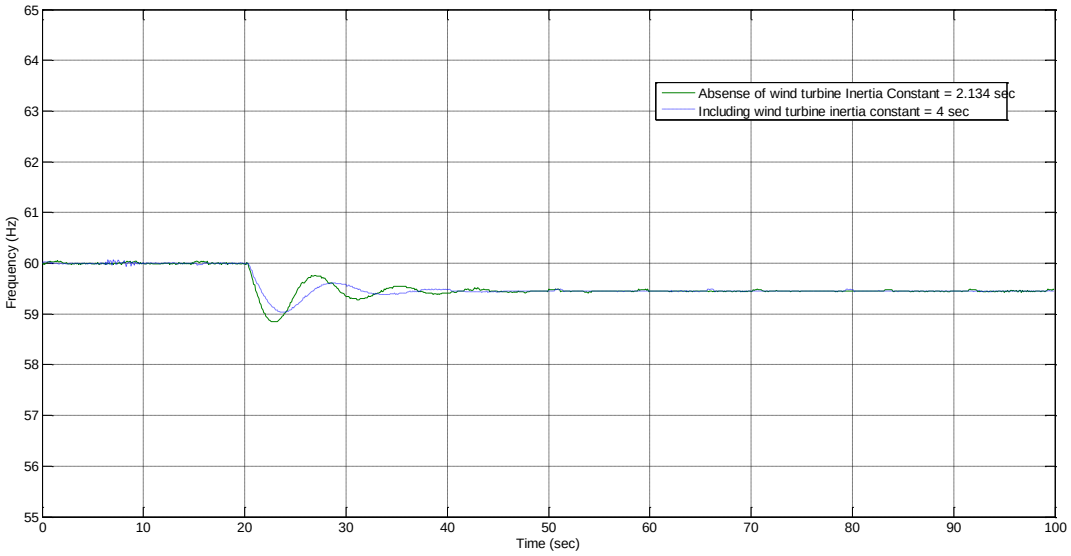

Figure 52 Aruba frequency behaviour for 8MW generation loss at 20 s with wind turbine inertia and absence of wind turbine inertia

For assumed unit commitment inertia constant of Aruba grid was 2.613 s, in this case maximum dynamic frequency drop reached to 58.846 Hz. When considering wind turbines in Aruba also providing inertia (wind farms will not be disconnected from grid even when frequency disturbance occurs) the grid maximum dynamic frequency drop recorded as 59.0356 Hz. Maximum dynamic frequency deviation of current Aruba's grid is 3.69% compare with nominal frequency of 60Hz. Maximum dynamic frequency deviation of current Aruba's grid with wind turbine inertia is 3.274% compare with nominal frequency of 60Hz.

It is evident that increase in inertia reduces dynamic frequency deviations. In other words, increase in grid inertia resists the change in frequency, thus stability of grid is also increases. It agreed that in real time frequency drop less than certain value for example 59 Hz will trigger protective action such as load shedding. However in simulation protection action were not considered.

4.5. Hardware limitation

Mechanical capability of motor generator setup to change its frequency of operation with respect to time is discussed in this section. This effect can be called as mechanical limitation or machine performance limitation.

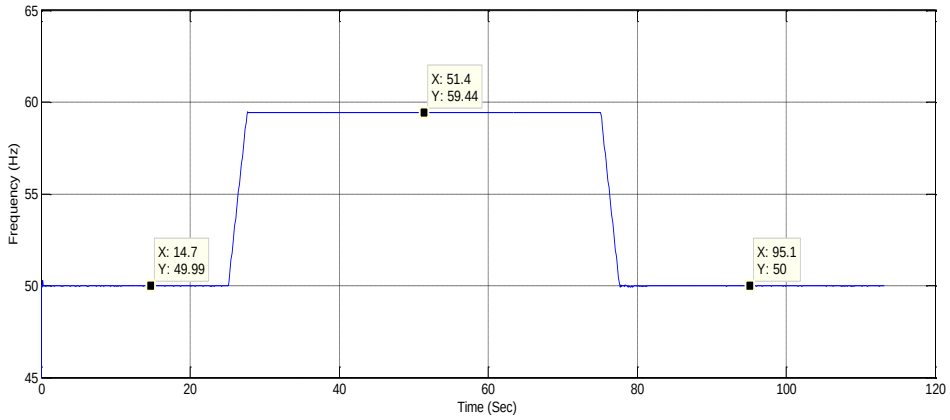

Figure 53 Mechanical limitation

In this section, the mechanical limitation that experienced during experiments was discussed. Though current experiments were not constrained by this mechanical limitation. It is necessary to analyse the machine performance to avoid instability in future experiments.

The maximum slew rate for frequency change with respect to time is limited by 3.73Hz/s. Figure 53 is the result of open loop test in which ~25sec generator frequency raised from 50 to 60Hz. In this experiment neither inertia nor primary control were used. Hence rate of change of frequency depends on machine intrinsic design and motor drive characteristics. Same procedure was repeated for frequency change from 60Hz to 50Hz around 70s. In both cases it was found that machine performance is limited by factor of 3.73Hz/s. In future experiments, more complex power system will be developed. In that case, ROCF plays an important role in activation of number of circuit breakers for protective action. Such scenarios can be developed using OPALRT® or RTDS®. In future experiments, experiments exceed machine mechanical performance limit, system will be instable.

5. Future Work: Micro Grid

In this chapter detailed description of proposal for future work on PHIL experiment, to create a micro grid laboratory is discussed. The relation between current thesis studies and future proposal for micro grid environment are also discussed in this chapter.

5.1. Importance of micro grid

'Amidst the blackouts that came with Hurricane Sandy's East Coast assault, a few islands of light and heat stood out. From the suburbs of Maryland and bucolic Princeton, N.J. to the hardest-hit sections of downtown Manhattan, microgrids -- building or campus-wide backup power systems that can disconnect, or "island" from the grid -- stood firm during the storm, proving their value in a disaster.' [24]

The above mentioned news report proves the reliability created by micro grid during Hurricane Sandy. It proves though main grid fails, micro grid can go into island operation and provide continuous power supply. Micro grid encourages integration of renewable energy by managing it both economically and technically. In micro grid, continuous power supply need to be assured in case of main grid failure; which can be provided either by storage or quick reacting power generation facilities. Interestingly, the same facility can be used to support high penetration of DER.

Improvement of electricity transmission infrastructure is slower than load growth. Thus introduces power quality problems. When power quality problem occurs in main grid, micro grid can go into island operation and assures power quality to customers. Investment in smart grid are increasing, even United States Army investing on micro grid [20].

5.1.1. Energy efficiency drivers for micro grid

- Number of micro grid facility includes CHP that is heat driven. Local generation of heat from CHP reduces losses, which is present in distribution network of district heating system.
- Micro grid encourages local power generation thus reduces losses occurred in Transmission.
- Micro Grid is capable of providing 'mission critical' status to its consumers.
- It can support main grid for active and reactive power support thus generates revenues.

5.2. Micro grid concept

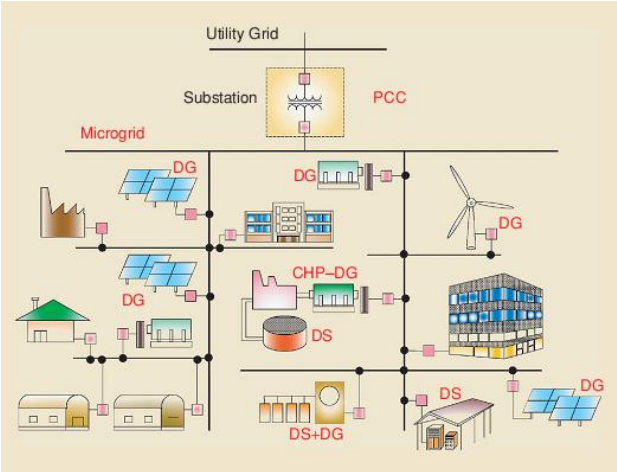

Figure 54 Typical micro grid/ grid segment

As shown in figure 54, grid segment or micro grid is a micro power system consists of communication architecture [38][35], different kind of loads and different kind of generation sources (PV, CHP, FC, micro turbine) located downstream of distribution substation.

Reasons for micro grid island operation can be

- Faults or Power Quality problems in main utility grid
- Planned maintenance activity in main utility grid or unexpected utility grid failure e.g.; Hurricane.

5.3. Conceptual design of future micro grid laboratory

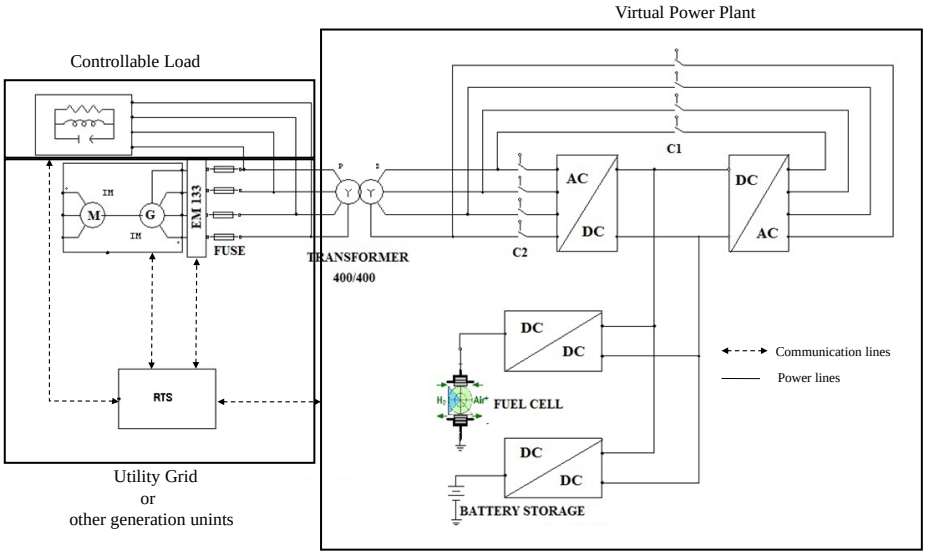

Figure 55 Conceptual design for micro-grid laboratory setup

The design of micro grid laboratory need to be proceeded in three dimensions [3].

1. Control Design
2. Hardware Configuration
3. Functionality

In this thesis, more focus is made on Hardware configuration section and control design for micro grid laboratory.

Figure 55 is the conceptual design for future micro grid laboratory setup. Power flow in this micro grid setup can reach up to ~35 kW. Because, motor generator set can provide power of 20 kW and Virtual power plant capable of providing power of 10 kW. The number of experiments can be implemented in this setup such as,

Case1: Using Triphase-Virtual Power Plant, providing active and reactive power support to utility grid. In this experiment motor-generator setup will act as utility grid [39].

Case2: Power Quality experiments like harmonic mitigation, voltage fluctuation control and flicker control.

Case3: Developing and configuring micro grid management system in island mode operation. In this mode motor generator can be modelled to emulate conventional generation units or to emulate of wind energy.

Case4: Development and testing of market concepts for fast and slow market for real&reactive power supply to utility.

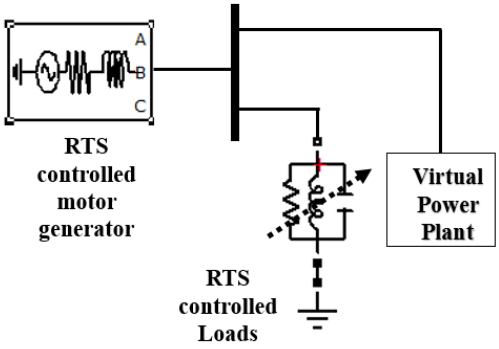

Figure 56 Basic components of micro grid laboratory proposal

In figure 56, three foundation blocks for proposed micro grid laboratory design were expressed. In which, RTS controlled motor generator and RTS controlled loads were developed already in this thesis work.

5.3.1. RTS controlled power source

Hardware configuration and control design for micro grid are introduced in this section. 52.5 kVA generator will be driven by 22 kW motor. This generator can be modelled as simple generator as in figure 56 or more complex grid such as figure in Appendix A.11. For more complex grid system computing power of existing real time computer may not be sufficient. Parallel real time simulators such as OPAL-RT® or RTDS® can be used.

5.3.2. RTS controlled Loads

Basic RTS controlled resistive loads were designed for this thesis work. More details regarding RTS controlled loads can be found in section 4.3.2.1. More complex controllable loads will be developed in future.

5.3.3. Virtual power plant using Triphase

It was suggested to use Triphase to create a Virtual Power Plant (VPP). With the help of VPP distributed energy resources can be controlled/managed by control algorithm. Controlling of DER results in virtual power plant scenario. More detailed study can be done in the VPP in future.

The DER connected in VPP can act in three different modes [9].

Grid forming

In this mode DER and interface, will act as constant voltage source with fixed frequency. It plays important role in island operation mode of micro grid.

Grid feeding

Irrespective of grid status, this kind DER either supply or consume power by its own need. VPP may get into this mode, when connected with utility grid and making energy trade.

Grid supporting

In this mode VPP will exchange power with grid for improving stability or power quality of grid.

5.4. Power balancing concept

In this section a basic proposal for power management of VPP is discussed. [32] study used as basic concept for this section.

As in figure 55, it is assumed VPP is supplied with battery storage and fuel cell. In which battery storage used for fast response and Fuel is used for slow responses. Power flow balancing for VPP in grid feeding mode can be found in equation 5.1.

$$P_{vppg}(t) = P_{FC}(t) + P_{batt}(t) - P_{load} \tag{5.1}$$

P_{vppg} denotes power exchange between VPP and grid segment; P_{FC} will act as slow response unit and P_{batt} is battery power output that act as fast response unit.

Currently frequency stability is responsibility of TSO. TSO maintains contracts with various energy generators for maintaining supply-demand balance. In future, DER will produce significant amount of energy. There will be possibilities that VPP will support grid stability. This mode called as grid supporting mode. In this mode DSO or aggregator provide set point ($P_{vppg,set}$) for energy exchange between VPP and utility grid.

By controlling $P_{vppg,set}$ power exchange between utility grid and VPP can be controlled. In future work, proposals for electricity power bidding can be developed for market based power management. Also it is interesting to analyse possibilities of integrating well proven powermatcher software for managing VPP.

In grid supporting mode, VPP need to be controlled in two aspects; which are

- Long Term Balance
- Short Term Balance

Long Term Balance

Fuel cell will be used for long term power supply to grid. Because, fuel cell are high efficient than other power generation methods.

Power balance P_{load} and P_{batt} are known values and DSO will provide $P_{vppg,set}$ hence set point for fuel cell operation can be found in equation 5.2,

$$P_{FC\_set} = P_{vppg,set}(T) - P_{batt}(T) + P_{load}(T) \quad (5.2)$$

P_{FC_set} will be used to control power output of fuel cell.

Short Term Balance

Short term instability occurs between VPP and utility grid due to many reasons such as ramp time of fuel cell or grid frequency fluctuation.

The short term power fluctuation can be managed by battery's fast charging or fast discharging. The operational set point for battery can be found in equation 5.3.

Short Term/instantaneous stability of VPP can be maintained by RTS monitored battery system[1]; the equation for this operation as follow

$$P_{batt}(t) = P_{vppg,set}(t) - P_{FC}(t) + P_{load}(t) \quad (5.3)$$

[1] Fast charge or discharge cycle may affect the life time of battery. Possibilities of replacing batteries with super capacitors need to be studied.

5.5. Relation between this thesis and the proposal

Majority of the equipment needed to develop micro grid laboratory for proposed concept were analysed during the course of this thesis work. As explained section 5.3, the hardware configuration dimension of micro grid laboratory development has been successfully initiated by configuring and procuring motor generator setup, real time computer, controllable load, power quality measurement smart meter SATEC EM133® and battery storage. Control dimension of micro grid development has been successfully initiated by controlling RTS, motor generator setup and controllable loads for this thesis work.

The micro grid proposal may be presented to I-Balance, Innovatiecontract smart grid by Agentschap NL, Ministry of Economic Affairs, which motivated my thesis work since from beginning.

6. Conclusion

Since PHIL experiment is a futuristic emerging technology in the field of power systems, a strategy to develop PHIL experiment has been developed. Emulation of power system in the PHIL experiment can be done by two methods - by power converters and motor-generator setup. Possibilities of using both methods were studied and motor-generator was chosen for power system emulation. Because, future PHIL experiment will use power converters for implementing virtual power plant concept.

In PHIL experiment, the simulation environment and hardware environment were implemented in real time using Engineering PC, Real Time PC, motor generator set and controllable loads. In the process of developing PHIL experiment, challenges such as controllable load design, communication, calibration, constrains and delays were solved. Controllable load was designed in such a manner so that it can be controlled in real time which is critical for demand side load control. Challenges of real time communication between computer and Beckhoff module were solved by Triphase BusXMLEditor. For PHIL experiment to be successful, a calibrated power measurement was necessary, which was achieved by finding RMS value with accurate offset. Calibration of frequency measurement was achieved by using filters and slow logging techniques. Stability issues with PHIL experiment for current model was observed as slew rate higher than 0.5 Hz/s for current model and mechanical slew rate constrain for current PHIL experiment setup was observed as 3.7 Hz/s. Key delay elements in PHIL experiment were identified- some of which are Ethernet speed 50 ms, load switching time ~25 ms, PLL measurement cycle ~100 ms.

The main two phases in development of PHIL experiment are Simulink model development and laboratory tests. Simulink model was developed to emulate effect of inertia, self-regulating load, network power frequency characteristics and primary reserve deployment time on primary frequency control of a grid segment. The problem of primary reserve deployment time for grid segment was analysed and a solution is provided. First order system was used to simulate primary reserve deployment time as per ENTSO-E guidelines. Test cases to study inertia, self-regulating load and primary control were developed and tested. The abovementioned Model was able to pass all test results which are discussed in chapter 3. The Simulink model was implemented in real time using real time computer/Linux PC.

A successful basic PHIL experiment was conducted using two ~3kW resistive loads which was consider as Hardware Under Test (HUT). In the experimental setup HUT and emulated power system makes a closed loop. The power flow change in HUT affected the frequency output of emulated power system via generator. Change in frequency for change in power of the HUT in the loop proves the validity of PHIL experiment.

The motivation of this thesis was developing emulated power system to mimic the disturbance of grid segment, to study the behaviour of future power system equipment during frequency disturbance. The effectiveness of model was compared with 04 Nov 2006 Europe grid disturbance, which resulted in the need to develop a more detailed model for accurate emulation of 2006 grid disturbance. HIL experiment was conducted to emulate frequency behaviour of Aruba's grid for using wind turbine inertia as a stability solution, which found that inertia constant of Aruba can be increased by 1.4 s from current inertia constant. It was found that by using wind turbine inertia, maximum dynamic frequency deviation of Aruba grid for loss of 8 MW unit can be reduced to 58.85 Hz compare with 59.04 Hz of current value.

A proposal was prepared for a future micro grid laboratory setup. Micro grid laboratory development requires knowledge in the field of real time control of emulated power system and load. This Thesis successfully conducted experiments for emulating real time power system and real time control of load. Thus knowledge necessary for developing micro grid laboratory set up was gathered during this thesis study. Also, hardware configuration and control for development of micro grid laboratory were initiated successfully by procuring controllable loads, battery storage and smart meter. As complex model may be developed for micro grid laboratory setup, RTS with parallel central processing units such as OPAT-RT or RTDS may need to be procured for high computing power.

7. Bibliography

[1] (2010). Retrieved from www.thewindpower.net: http://www.thewindpower.net/windfarm_en_15255_aruba.php

[2] A joint EURELECTRIC - ENTSO-E response paper. (2011). *Determining frequency deviations - root causes and proposals for potential solutions.*

[3] A. Ishchenko, W. K. (2009). *Control Aspects and the Design of a Small-Scale Test Virtual Power Plant.* IEEE.

[4] Ahmasd Mosavi, D. T. (n.d.). Retrieved from www.eng.uwo.ca: http://www.eng.uwo.ca/people/tsidhu/Documents/Course%20Project%20-%20ES%20586B.pdf

[5] Alan Mullane, G. B. (n.d.). *Kinetic energy and frequency response comparisons for renewable generation systems.* University College Dublin: Retrieved from http://ieeexplore.ieee.org/stamp/stamp.jsp?tp=&arnumber=1600525

[6] Amine Yamane, W. L. (2011). *A Smart Distribution Grid Laboratory.* Opal-RT Technologies Inc, Osaka University, NF Corporation .

[7] Andersson, G. (2012). Dynamics and Control of Elelctric Power Systems.

[8] Bouscayrol, A. (2008). *Different types of Hardware-In-the-Loop simulation for electric drives.* University of Lille, L2EP Lille, USTL, 59 655 Villeneuve d'Ascq, France.

[9] Brabandere, K. D. (2006). *PhD Thesis, Volatage and Frequency Droop Control in Low Voltage Grids by Distributed Generators with Inverter Front-End.* Katholieke Universiteit Leuven.

[10] Christoph Molitor, A. B. (2013, March). Multiphysics Test Bed for Renewable Energy Systems in Smart Homes. *IEEE Transaction on Industrial Electronics*, pp. VOL 60, NO. 3.

[11] ENTSO-E. (2011). Statistical Year Book 2011.

[12] ENTSO-E. (2012). *Operational Reserve AD HOC Team Report Final Version.*

[13] ENTSO-E. (24.06.2004 v2.5). *I - Introduction to the UCTE Operational Handbook (OH) [E].*

[14]ENTSOE Appendix-1, . (2004). *Load-Frequency Control and Performance.*

[15]ENTSO-E. (n.d.). Policy 1 - Load Frequency Control and Performance.

[16]*entsoe.eu*. (n.d.). Retrieved from https://www.entsoe.eu/about-entso-e/working-committees/system-operations/regional-groups/

[17]European Commission, Directorate-General for Energy and Transport. (2007). *European Ennergy and Transport, Trends to 2030 - Update 2007.* European Commission.

[18]European Regulators' Group for Elelctricity and Gas. (2007). *The lessons to be learned from the large disturbance in the European power system on the 4th of November 2006.* Brussels.

[19]Fernando D. Bianchi, H. D. (2007). *Wind Turbine Control Systems.* Springer.

[20]Fool, B. W. (2013). Retrieved from www.dailyfinance.com: http://www.dailyfinance.com/2013/05/10/microgrids-for-military-bases-to-surpass-377-milli/

[21]Frunt, J. (2011). *Ph.d Dissertion, Analysising Balancing Requirements in Future Sustainable and Reliable Power System.*

[22]*http://portal.triphase.eu/*. (n.d.).

[23]IEA. (2012). *CO2 emissions from fuel combustion Highlights.*

[24]JOHN, J. S. (2012, November 20). Retrieved from https://www.greentechmedia.com: https://www.greentechmedia.com/articles/read/how-microgrids-helped-weather-hurricane-sandy

[25]Joon-Young Park, J.-K. L.-Y.-S.-J. (2010). Design of Simulator for 3MW Wind Turbine and Its Condition Monitoring System. *Proceedings of the International MultiConferencec of Engineers and Computer Scientists 2010 Vol II.* Hong Kong.

[26]Kuhnke. (n.d.). *www.kuhnke.co.uk.* Retrieved from http://www.kuhnke.co.uk/pdf/relays/114.pdf

[27]Kundur, P. (n.d.). *Power System Stability and Control.* Chapter 11: Mc Graw-Hill, Inc.

[28]Nederland, T. N.-B. (2011). *Imbalance Management TenneT Analysis report* . E-Bridge & GEN Nederland .

[29]P. Crolla, A. R. (2011). Methodology for testing loss of mains detetion algorithms for microgrids and distributiuon generation using real-time power hardware-in-the-loop based

technique. *8th International Conference on Power Electronics*, (pp. 833-838). The Shilla Jeju, Korea.

[30]P. Kotsampopoulos, V. G. (2012). *Design, development and operation of a PHIL environment for Distribution Energy Resources.* National Technical University of Athens.

[31]Pannier, J. (2012, July 04). *portal.triphase.eu*. Retrieved from http://portal.triphase.eu/_/system-overview/real-time-control-r16

[32]Peng LI, P. D. (2009). Participation in Fequency Regulation Control of a Resilient Microgrid for a Distribution Network. *International Journal of Integrated Energy Systems*, 1-5.

[33]Pieter Tielens, D. V. (n.d.). Grid Inertia and Frequency Control in Power Systems with High Penetration of Renewables.

[34]Products, E. T.-D. (2013, February 1). *http://publications.elia.be.* Retrieved from http://publications.elia.be/upload/UG_upload/QUTHEWRGFC.pdf

[35]Rachid BELFKIRA, O. H. (n.d.). Optimal sizing of stand-alone hybrid wind/PV system with battery storage. University of Le Havre, 25 rue Philippe Lebon, BP 540, France.

[36]Schneider Electric. (n.d.). *Chracteristics TeSys contactors MOdel d.* Retrieved from http://www.datasheetarchive.com/LC1Dt25-datasheet.html

[37]Shahram Karimi, P. P. (2010, April). An HIL-Based Reconfigurable Platform for Design, Implementation, and Verification of Electrical System Digital Controllers. *IEEE TRANSACTIONS ON INDUSTRIAL ELECTRONICS*, pp. VOL 57,NO. 4.

[38]Stavros Lazarou, R. T. (n.d.). *A Smart Grid Simulation Centre at the Institute for Energy and Transport - Model validation of VSC - MTDC for integration of offshore wind energy.*

[39]T. Vu Van, K. V. (n.d.). *Virtual Synchronous Generator: An Element of Future Grids.*

[40]TenneT. (n.d.). *energieinfo.tennet.org.* Retrieved from http://energieinfo.tennet.org/Production/InstalledCapacity.aspx

[41]UCTE. (2007). *Final Report System Disturbance on 4 November 2006.*

[42]Vasileios Karapanos, S. d. (2011). *Real Time Simulation of a Power System with VSG Hardware in the Loop.* Delft University of Technology, the Netherlands.

[43]Vestas. (2013). Retrieved from http://www.vestas.com/en/wind-power-plants/procurement/turbine-overview/v90-3.0-mw.aspx#/vestas-univers

[44]Water-En Energiebedrijf Aruba N.V. (n.d.). Retrieved from http://www.webaruba.com/: http://www.webaruba.com/en/productsequipment/products/electricity.html

[45]*www.webaruba.com/*. (2013). Retrieved from http://www.webaruba.com/en/productsequipment/equipment/turbine-generator.html

[46]Yann G. Rebours, S. M. (2007). A Survey of Frequency and Voltage Control Ancillary Services—Part I: Technical Features. *IEEE TRANSACTIONS ON POWER SYSTEMS*, 350-357.

Nomenclature

7.1. List of Acronyms

B-VCA	Basic knowledge of Safety, Health and the Environment Certificate
CHP	Combined Heat and Power Generation
DER	Distributed Energy Resources
DG	Distribution Generation
DSO	Distribution System Operator
ENTSO-E	European Network of Transmission System Operators for Electricity
EPS	Emulated Power System
EU	European Union
FC	Fuel Cell
FCR	Frequency Containment Reserve
FPGA	Field Programmable Gate Array
FRR	Frequency Restoration Reserve
HIL	Hardware in the Loop
HUT	Hardware under Test
ICT	Information and Communication Technology
IP	Internet Protocol
PC	Primary Control
PHIL	Power Hardware in the Loop

PLC	Programmable Logic Controller
PLL	Phase Locked Koop
PV	Photo Voltaic
RECIP	Reciprocating Internal Combustion Engines
RMS	Root Mean Square value
ROCF	Rate of Change of Frequency
RR	Restoration Reserve
RTDS	Real Time Digital Simulator
RTS	Real Time System (computer)
SRL	Self-Regulating Load
TCP	Transmission Control Protocol
TSO	Transmission System Operator
UCTE	Union for the Coordination of the Transmission of Electricity
VPP	Virtual Power Plant

7.2. List of Symbols

H	Inertia Constant (s)
J	Moment of Inertia (kgm^2)
ms	milli Second
P	Power (p.u and W)
PgPC	primary reserve of generator (%)
S	Apparent Power (VA)
Sg	Generator Droop Constant (%)
SRLE	Self-Regulative Load Effect ($\frac{\%}{Hz}$)
T	Torque (p.u)
Ts	Model Sample Time (s)
λ	Network Power Frequency Characteristics ($\frac{W}{Hz}$)
ω	Rated Speed ($\frac{rad}{s}$)
ω	Rotor angular frequency of generator ($\frac{rad}{s}$)
f	Frequency (Hz)

7.3. List of Indices

$0m$	rated speed at zero second
i	i^{th} generator or i^{th} control area
0	nominal
$p.u.$	per unit
m	mechanical related parameter
e	electrical related parameter
B	base value
$L`$	Load
srl	self-regulating load effect
syo	whole synchronous area
mg	micro grid
FC	fuel cell
$batt$	battery
set	set value
$vppg$	between virtual power plan and utility grid
$vppg, set$	set value for power exchange between virtual power plan and utility grid

Appendix

A.1

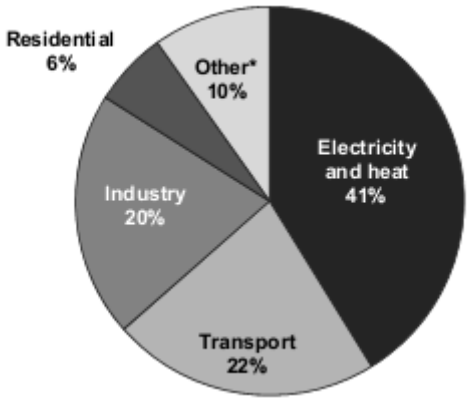

Figure World CO2 emission per sector in 2010 [23]

A.2

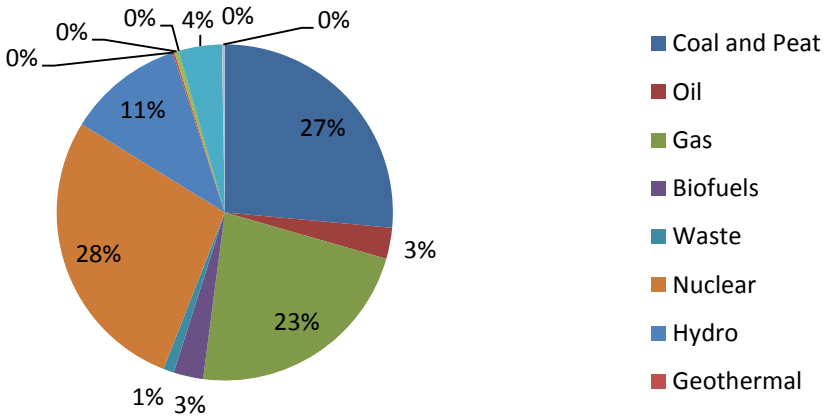

Figure Electricity production of EU-27 in 2009 [17]

A.3 Triphase Details

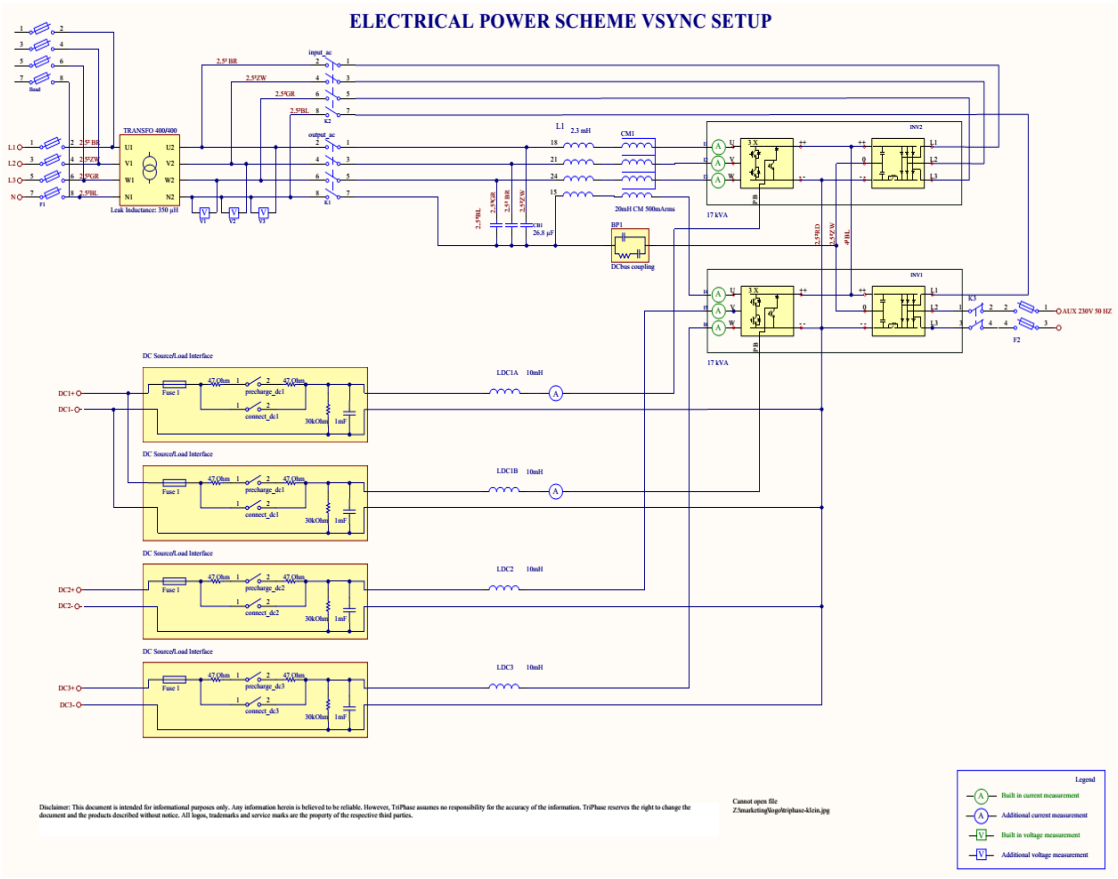

Figure Schematic of Triphase Power Diagram

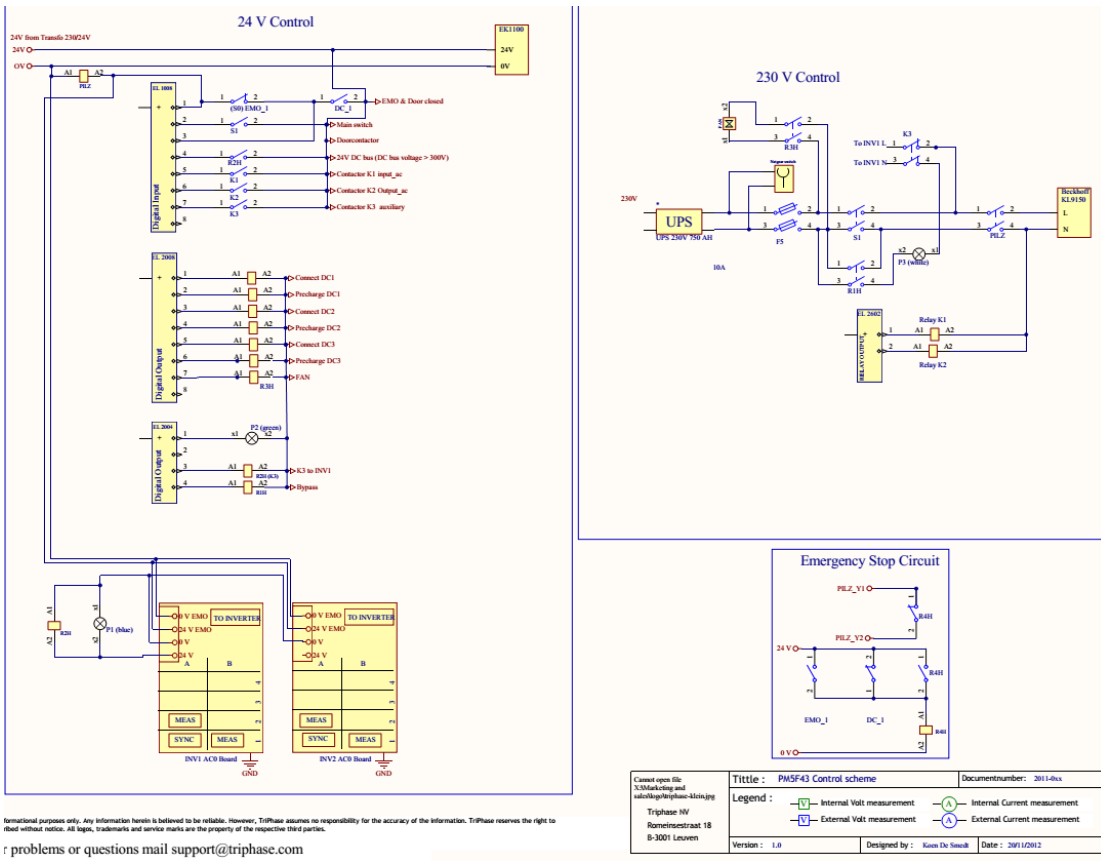

Figure Control Schematic of Triphase

Hardware Specifications

General	Auxiliaries supply voltage	230V AC, 50-60Hz
	Power Supply voltage	3 Phase 220-480 V_{RMS} [L-L], 50-60 Hz / 350-700 V_{DC}
	Switching frequency	8-16 kHz
	Maximum DC bus voltage	700 V
AC/DC	Output voltage	0-480 V_{RMS} [L-L]
	Output current	3 x 16 A_{RMS} / 3 x 24 $A_{RMS,peak(60s)}$
	Rated power	11 kVA / 15 kVA_{peak}(1)
	Fuses	3 x 25 A
DC/DC	Output voltage	3 x 100-650 V(2)
	Output current	3 x 16 A / 3 x 24 A_{peak}(1)
	Rated power	3 x 3.68 kW / 3 x 5 kW_{peak}(1)
	Fuses	3 x 2 x 25 A
Mechanical	Enclosure	Rittal TS8 1350 x 550 x 820 mm
	Construction	Powder Coated Steel
	Weight estimate	233 kg
	Cooling	Forced Convection
	Temperate Range	0-40 °C
	Maximum Humidity	80 % Non Condensing
Safety	Overvoltage Protection	Software configurable limit
	Overcurrent Protection	Software configurable limit
	Overtemperature Protection	Software configurable limit
	Emergency Button	On Cabinet Door(3)

(1) Peak values can be generated by the power module during max. 60 seconds per 600 seconds.
(2) maximum output voltage is DC-bus voltage - 50 V_{DC}
(3) External emergency button(s) available on request.

Figure Hardware Specifications

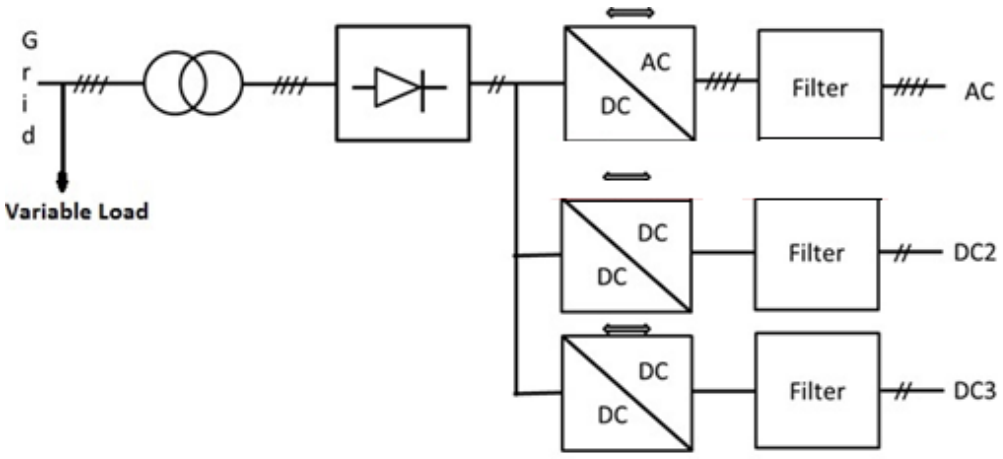

Figure Block Diagram of Triphase Hardware

Power Architecture of Triphase®

Triphase® is a fast prototyping module consist of two inverter modules, Isolation transformer, Soothing reactive components, external voltage and current measurement. As you can see in figure 'Schematic of Triphase Power Diagram' a Fuse named F1 is a physical contactor between main grid supply to cabinet. There is an isolation transformer is present to provide galvanic protection between Generator/Grid and Triphase® cabinet.

There are four external current and three external voltage measurement units are present inside Triphase® cabinet; which will be used to make Power Hardware in Loop experiment. More details regarding experimental setup will be discussed in later.

Important power electronics element in Triphase® is two full leg IGBTs and two half leg IGBTs. Using this version of Triphase® one neutral controlled three phase power source, one unidirectional DC power source, and two birectional DC storage or source can be developed.

K1, K2 and K3 are PLC controlled power switches. Here is a challenge. K1, K2 and K3 are power by PLC at the same time PLC need power supply which is being supplied by DC bus of Inverter and converter bus. This problem is solved by setting K3 as normally closed. So by normally closed DC bus will reach voltage around ~300Vdc.Once this DC bus is energised PLC board will be powered. PLC board can control contactors in controllable load centre or it can control speed of motor. Also it is important to note that with this 300Vdc it is advisable to generate three phase voltage source through inverter since it will overload K3 and its auxiliaries such that equipment will be damaged.

This K3 problem is conveyed to Triphase® engineer and he agreed it is an disadvantage and current system no longer uses DC bus of inverter instead they have separate AC/DC converter to energise PLC and measurement boards.

Triphase® is developed with watchdog protocols which make sure there is no damage occurs due to overcurrent or over voltage. There was a problem with inrush current in Transformer was overcome by developing soft starting of transformer. This soft starter in beginning bypass inrush current through high power resistor for about ~3sec then timer based relay redirect current through transformer such that inrush current is avoided. I helped Triphase® in building soft starter circuit for transformer.

3 ph utility connection can be used to boost DC voltage up to 720V. It is possible to provide or obstruct reactive power from grid via inverter connection. DC 2&3 are rated from 120V to 650V and current rating of 16A. Two inverters with rating of 17kVA are installed that has nominal current value as 16A per phase. Inverters are protected against over current, voltage and temperature. Also emergency stop and door position detection act as watchdog that provide safety.

A.4 XML file of field bus

```
<?xml version="1.0" encoding="utf-8"?>
<fieldbusses>
  <fieldbus name="virtual" type="Virtual">
    <registers>
      <register name="lsr">
        <read state="1"/>
      </register>
      <register name="_ecpe_disable_">
        <read state="0"/>
      </register>
    </registers>
  </fieldbus>
  <fieldbus filename="rteth0" name="ethercat" period_us="50000" type="EtherCat">
    <devices><!-- 230 V -->
      <device name="EL1008-1" position="1" product_code="0x03F03052"
vendor_id="0x00000002"/>
      .
.
.
.
```

A.5 Primary Control mechanism of various Grid [16][46]

TABLE III
TECHNICAL COMPARISON OF PRIMARY FREQUENCY CONTROL PARAMETERS IN VARIOUS SYSTEMS

	NERC	UCTE	DE	FR	ES	NL	BE	GB
References	[24], [25], [26]	[29], [37]	[20], [21]	[18],[19]	[34]	[27], [28], [29]	[17]	[22], [23]
Full availability	No rec.	≤ 30 s	≤ 30 s	≤ 30 s	≤ 30 s	≤ 30 s	≤ 30 s	Pri.: ≤ 10 s Sec.: ≤ 30 s Hi.: ≤ 10 s
Deployment end	No rec.	≥ 15 min	≥ 15 min	≥ 15 min	≥ 15 min	≥ 15 min	≥ 15 min	Pri.: ≥ 30 s Sec.: ≥ 30 min Hi.: as long as required
Frequency characteristic requirement	10 %of the balancing authority's estimated yearly peak demand/Hz	20,570 MW/Hz	≈ 4,200 MW/Hz	≈ 4,200 MW/Hz	≈ 1,800 MW/Hz	≈ 740 MW/Hz	≈ 600 MW/Hz	Variable ≈ 2,000 MW/Hz
Droop of generators	5 % in 2004; no rec. anymore	No rec.	No rec.	3-6 %	≤ 7.5 %	5-60 MW: 10 % > 60 MW: 4-20 %	No rec.	3-5 %
Is an adjustable droop compulsory?	No rec.	No rec.	Yes	Yes	No rec.	5-60 MW: No rec. > 60 MW: Yes	No	Yes
Accuracy of the frequency measurement	No rec.	Within ± 10 mHz	Within ± 10 mHz	No rec.	No rec.	No rec.	Within ± 10 mHz	No rec.
Controller insensitivity	T: ± 36 mHz in 2004; no rec. anymore NI: No rec. I: No rec.	T: ± 10 mHz NI: No rec. I: should be compensated within the zone	T: ± 10 mHz NI: No rec. I: ± 0 mHz	T: ± 10 mHz NI: No rec. I: should be compensated within the zone	T: ± 10 mHz NI: No rec. I: ± 0 mHz	5-60 MW: T: ± 150 mHz; NI: No rec.; I: No rec. > 60 MW: T: ± 10 mHz; NI: ± 10 mHz; I: ± 0 mHz	T: ± 10 mHz NI: ± 10 mHz I: No rec.	T: ± 15 mHz NI: No rec. I: No rec.
Full deployment for or before a deviation of:	No rec.	± 200 mHz	± 200 mHz	± 200 mHz	± 200 mHz	5-60 MW: 30 % for ± 150-200 mHz > 60 MW: 70 % for ± 50-100 mHz	± 200 mHz	Pri.: -800 mHz Sec.: -500 mHz Hi.: +500 mHz

No rec.: no recommendation; Pri., Sec. or Hi.: primary, secondary or high frequency response; I: intentional; NI: non intentional; T: total.

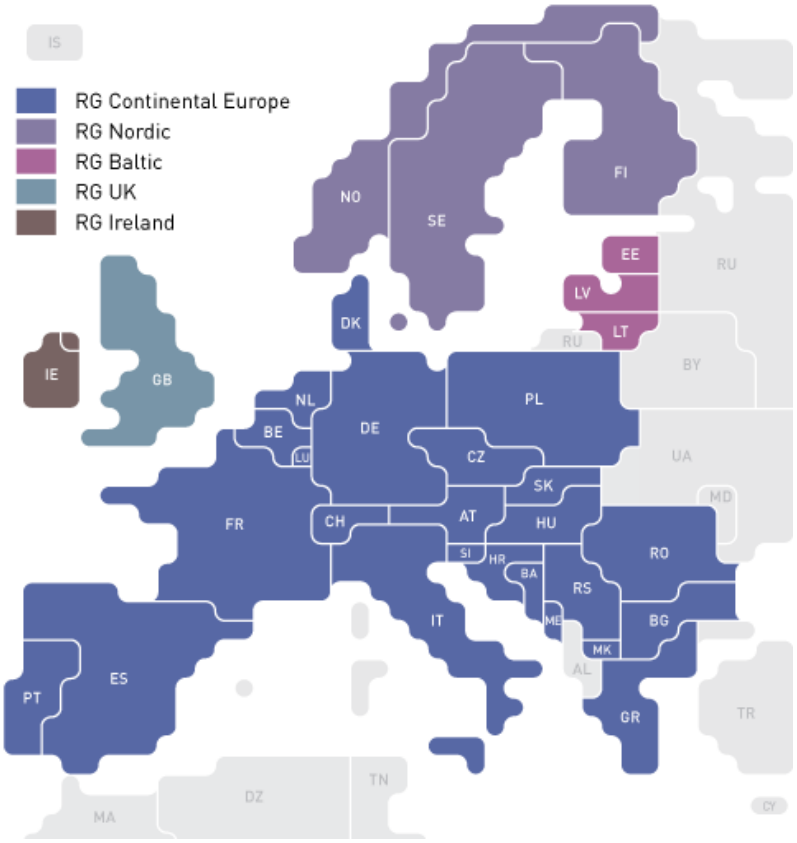

Figure Synchronous areas

A.6 B-VCA Diploma

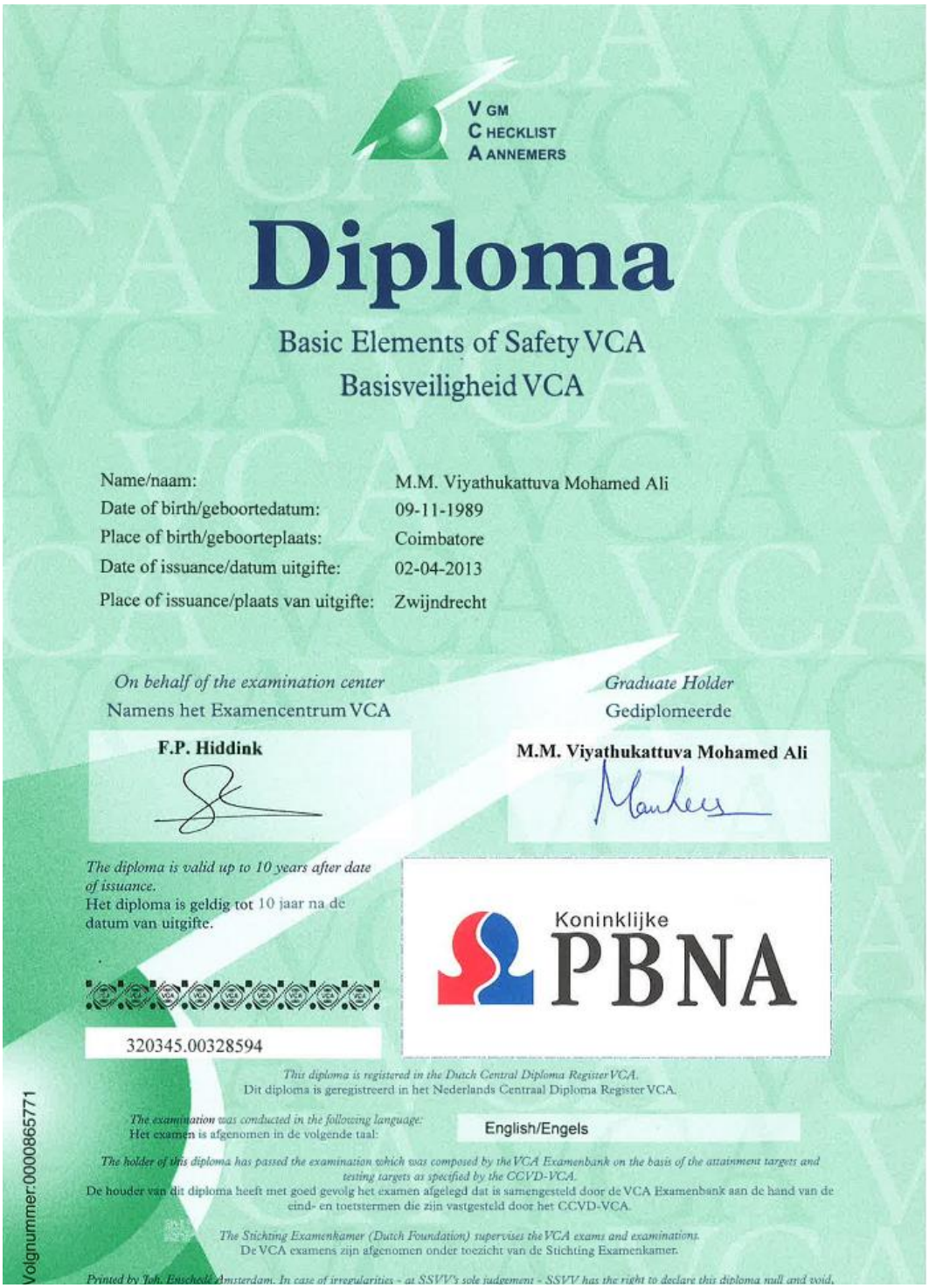

VGM
CHECKLIST
AANNEMERS

Diploma

Basic Elements of Safety VCA
Basisveiligheid VCA

Name/naam:	M.M. Viyathukattuva Mohamed Ali
Date of birth/geboortedatum:	09-11-1989
Place of birth/geboorteplaats:	Coimbatore
Date of issuance/datum uitgifte:	02-04-2013
Place of issuance/plaats van uitgifte:	Zwijndrecht

On behalf of the examination center
Namens het Examencentrum VCA

F.P. Hiddink

Graduate Holder
Gediplomeerde

M.M. Viyathukattuva Mohamed Ali

The diploma is valid up to 10 years after date of issuance.
Het diploma is geldig tot 10 jaar na de datum van uitgifte.

320345.00328594

Koninklijke PBNA

This diploma is registered in the Dutch Central Diploma Register VCA.
Dit diploma is geregistreerd in het Nederlands Centraal Diploma Register VCA.

The examination was conducted in the following language:
Het examen is afgenomen in de volgende taal: English/Engels

The holder of this diploma has passed the examination which was composed by the VCA Examenbank on the basis of the attainment targets and testing targets as specified by the CCVD-VCA.
De houder van dit diploma heeft met goed gevolg het examen afgelegd dat is samengesteld door de VCA Examenbank aan de hand van de eind- en toetstermen die zijn vastgesteld door het CCVD-VCA.

The Stichting Examenkamer (Dutch Foundation) supervises the VCA exams and examinations.
De VCA examens zijn afgenomen onder toezicht van de Stichting Examenkamer.

Printed by Joh. Enschedé Amsterdam. In case of irregularities - at SSVV's sole judgement - SSVV has the right to declare this diploma null and void.

Volgnummer:0000865771

Appendix A.7

Technical data	EL4004 | ES4004
Connection technology	2-wire, single-ended
Number of outputs	4
Power supply	24 V DC via power contacts
Signal voltage	0…10 V
Distributed clocks	yes
Distributed clock precision	<< 1 µs
Load	> 5 kΩ (short-circuit-proof)
Output error	< 0.1 % (relative to end value)
Resolution	12 bits
Electrical isolation	500 V (E-bus/signal voltage)
Conversion time	~ 250 µs
Current consumption power contacts	typ. 25 mA
Current consumption E-bus	typ. 140 mA
Bit width in the process image	4 x 16 bit AO output
Special features	Optional watchdog: user-specific output value with ramp; user synchronisation can be activated
Weight	approx. 85 g
Operating/storage temperature	0…+55 °C/-25…+85 °C
Relative humidity	95 %, no condensation
Vibration/shock resistance	conforms to EN 60068-2-6/EN 60068-2-27
EMC immunity/emission	conforms to EN 61000-6-2/EN 61000-6-4
Protect. class/installation pos.	IP 20/variable
Pluggable wiring	for all ESxxxx terminals
Approvals	CE, UL, Ex

Appendix A.8

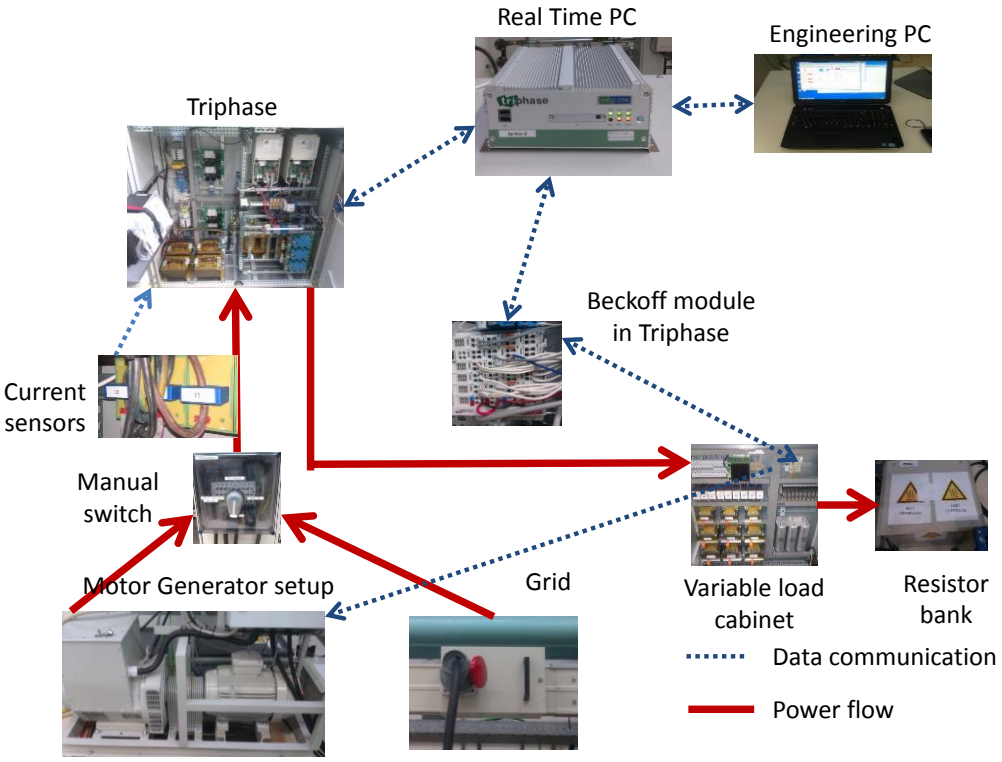

Figure PHIL experiment

Appendix A.9 Aruba overall installed capacity [45]

Generator Type	Capacity
3 × 33 MW Turbine Generator	99 MW
2 × 35 MW Turbine Generator	70 MW
6 × 8 MW RECIP Generator	48 MW
4 × 11.3 MW RECIP Generator	45.2 MW
GasTurbine	22 MW
Wartsila Diesel	6.2 MW
Vader Piet wind park	30 MW
Island Installed Capacity	320.4 MW

Appendix A.10 Inertia Constant for different type of Generation Units [5], [33]

Type	Fuel	Min Power(MW)	Max Power(MW)	Inertia Constant (s)
Steam	Oil	58	130	4
Steam	Oil	32	60	3.3
Steam	Oil	32	60	3.3
CCGT	Gas	45	115	4.3
Combustion	Oil	6	16.7	3.5
Gas	Gas	40	120	5
Gas	Gas	20	90	5

Type	H(s)
Thermal Unit	
3600 r-min (2-pole)	2.5 to 6.0
1800 r-min (4-pole)	4.0 to 10.0
Hydraulic unit	2.0 to 4.0

Appendix A.11 Complex Power System Model [6]